Department of Medicine Faculty Papers   Department of Medicine

8-20-2014

Adrenergic signaling regulates mitochondrial Ca2+ uptake through Pyk2-dependent tyrosine phosphorylation of the mitochondrial Ca2+ uniporter.

Jin O-Uchi
Department of Medicine, Jefferson Medical College, Thomas Jefferson University

Bong Sook Jhun
Department of Medicine, Jefferson Medical College, Thomas Jefferson University

Shangcheng Xu
Department of Anesthesiology and Pain Medicine, Mitochondria and Metabolism Center, University of Washington

Stephen Hurst
Department of Medicine, Jefferson Medical College, Thomas Jefferson University

Anna Raffaello
Department of Biomedical Sciences, University of Padua, CNR Neuroscience Institute

See next page for additional authors

Recommended Citation

Authors

Jin O-Uchi, Bong Sook Jhun, Shangcheng Xu, Stephen Hurst, Anna Raffaello, Xiaoyun Liu, Bing Yi, Huiliang Zhang, Polina Gross, Jyotsna Mishra, Alina Ainbinder, Sarah Kettlewell, Godfrey L Smith, Robert T Dirksen, Wang Wang, Rosario Rizzuto, and Shey-Shing Sheu

Discoveries

Forum Original Research Communication

Adrenergic Signaling Regulates Mitochondrial Ca^{2+} Uptake Through Pyk2-Dependent Tyrosine Phosphorylation of the Mitochondrial Ca^{2+} Uniporter

Jin O-Uchi,[1,][*] Bong Sook Jhun,[1,][*] Shangcheng Xu,[2] Stephen Hurst,[1] Anna Raffaello,[3] Xiaoyun Liu,[2] Bing Yi,[1] Huiliang Zhang,[2] Polina Gross,[1] Jyotsna Mishra,[1] Alina Ainbinder,[4] Sarah Kettlewell,[5] Godfrey L. Smith,[5] Robert T. Dirksen,[4] Wang Wang,[2] Rosario Rizzuto,[3] and Shey-Shing Sheu[1]

Abstract

Aims: Mitochondrial Ca^{2+} homeostasis is crucial for balancing cell survival and death. The recent discovery of the molecular identity of the mitochondrial Ca^{2+} uniporter pore (MCU) opens new possibilities for applying genetic approaches to study mitochondrial Ca^{2+} regulation in various cell types, including cardiac myocytes. Basal tyrosine phosphorylation of MCU was reported from mass spectroscopy of human and mouse tissues, but the signaling pathways that regulate mitochondrial Ca^{2+} entry through posttranslational modifications of MCU are completely unknown. Therefore, we investigated α_1-adrenergic-mediated signal transduction of MCU posttranslational modification and function in cardiac cells. **Results:** α_1-adrenoceptor (α_1-AR) signaling translocated activated proline-rich tyrosine kinase 2 (Pyk2) from the cytosol to mitochondrial matrix and accelerates mitochondrial Ca^{2+} uptake *via* Pyk2-dependent MCU phosphorylation and tetrametric MCU channel pore formation. Moreover, we found that α_1-AR stimulation increases reactive oxygen species production at mitochondria, mitochondrial permeability transition pore activity, and initiates apoptotic signaling *via* Pyk2-dependent MCU activation and mitochondrial Ca^{2+} overload. **Innovation:** Our data indicate that inhibition of α_1-AR-Pyk2-MCU signaling represents a potential novel therapeutic target to limit or prevent mitochondrial Ca^{2+} overload, oxidative stress, mitochondrial injury, and myocardial death during pathophysiological conditions, where chronic adrenergic stimulation is present. **Conclusion:** The α_1-AR-Pyk2-dependent tyrosine phosphorylation of the MCU regulates mitochondrial Ca^{2+} entry and apoptosis in cardiac cells. *Antioxid. Redox Signal.* 21, 863–879.

Introduction

MITOCHONDRIAL CA^{2+} homeostasis determines numerous cell functions, including energy metabolism, reactive oxygen species (ROS) generation, spatiotemporal dynamics of Ca^{2+} signaling, cell growth/development, and death (19, 24, 56, 57). The mitochondrial Ca^{2+} uniporter (mtCU), which is inhibited by lanthanides and ruthenium red (26), is the primary mechanism for mitochondrial Ca^{2+} influx in all cell types (8). Although functionally characterized

several decades ago (18, 56), the complete molecular identity of the mtCU has yet to be fully elucidated. However, groundbreaking studies recently uncovered the molecular identity of the mtCU pore (MCU), the coiled-coil domain-containing protein 109A (*CCDC109A*) (3, 14), as well as the regulatory proteins (56). These findings open up exciting new opportunities for using genetic approaches to elucidate mechanisms that regulate mitochondrial Ca^{2+} uptake in various cell types, including cardiac myocytes (17). For example, basal tyrosine phosphorylation of *CCDC109A* was

---

[1]Department of Medicine, Center for Translational Medicine, Jefferson Medical College, Thomas Jefferson University, Philadelphia, Pennsylvania.
[2]Department of Anesthesiology and Pain Medicine, Mitochondria and Metabolism Center, University of Washington, Seattle, Washington.
[3]Department of Biomedical Sciences, University of Padua and CNR Neuroscience Institute, Padua, Italy.
[4]Department of Pharmacology and Physiology, University of Rochester Medical Center, Rochester, New York.
[5]Institute of Cardiovascular and Medical Science, University of Glasgow, Glasgow, United Kingdom.
*These authors contributed equally to this work.

Innovation

This report is the first to show the regulation of mitochondrial Ca^{2+} uptake, reactive oxygen species generation, and cell death signaling *via* mitochondrial Ca^{2+} uniporter pore (MCU) posttranslational modification. Our data provide significant and broad implications for understanding the regulation of MCU in cell signaling across all cell types, including cardiomyocytes. In addition, the results from this study suggest that inhibition of MCU tyrosine phosphorylation represents a potential, novel therapeutic target to prevent mitochondrial Ca^{2+} overload, oxidative stress, and mitochondrial/cell injury.

reported from mass spectroscopy analyses of human and mouse samples (see online database PhosphoSitePlus) (33). However, specific signaling pathways that control mitochondrial Ca^{2+} entry through posttranslational modifications of MCU are completely unknown.

In cardiac cells, adrenoceptor (AR) stimulation, either through β- or α_1-ARs, is a main determinant of physiological and pathophysiological cell signaling, predominantly through serine/threonine kinases [*e.g.*, protein kinase A and Ca^{2+}/calmodulin-dependent protein kinase II (CaMKII)](55). In addition, we reported that protein tyrosine kinases (PTKs) are also activated during α_1-AR stimulation (α_1-ARS) in cardiac myocytes (54), and another report showed that a Ca^{2+}-dependent PTK named proline-rich tyrosine kinase 2 (Pyk2) is activated in response to α_1-ARS (27). Pyk2 is expressed abundantly in cancers (42, 42). However, a recent study using human tissue showed that Pyk2 is also highly expressed in the heart and significantly activated during heart failure (40). Moreover, several reports indicate that Pyk2 is not only localized in the cytosol, but also in mitochondria (1, 23). Therefore, we hypothesize that α_1-AR-Pyk2 signaling regulates mitochondrial Ca^{2+} entry through MCU tyrosine phosphorylation in cardiac cells.

In this study, we report that Pyk2 activated by α_1-AR signaling directly phosphorylates MCU, which enhances mitochondrial Ca^{2+} uptake by promoting MCU channel oligomerization and formation of tetrameric channels. Moreover, we demonstrate that α_1-ARS and Pyk2 activation initiates ROS production in mitochondria (mitochondrial ROS: mROS), the activity of mitochondrial permeability transition pore (mPTP), apoptotic signaling, and cardiomyocyte death. This study is the first to show the modulation of MCU by adrenergic signaling and the regulation of ROS generation and cell death signaling *via* a posttranslational modification of MCU in cardiac cell.

Results

### α_1-AR stimulation accelerates mitochondrial Ca^{2+} uptake

To explore whether adrenergic signaling regulates mitochondrial Ca^{2+} uptake in cardiac cells, we monitored changes in the mitochondrial matrix Ca^{2+} concentration ($[Ca^{2+}]_{mt}$) by expressing Mitycam, a mitochondria-targeted Ca^{2+}-sensitive inverse pericam (39, 53), in intact cardiac H9c2 myoblasts (Fig. 1). In this cell, Mitycam localized exclusively in mitochondria by cotransfecting with mitochondrial matrix-targeted RFP (53) (mt-RFP) (Fig. 1A, B). We observed the peak amplitude of the changes in Mitycam fluorescence (decrease in Mitycam fluorescence) to evaluate the magnitude of mitochondrial Ca^{2+} uptake (39, 53) (see also online Materials and Methods section). The changes in the cytosolic Ca^{2+} concentration ($[Ca^{2+}]_c$) were also monitored by Fura-red (53) (Fig. 1 and Supplementary Fig. S1; Supplementary Data are available online at www.liebertpub.com/ars). Mitycam responded to elevations in $[Ca^{2+}]_{mt}$ in response to $[Ca^{2+}]_c$ elevations induced by an inhibitor of the sarco/endoplasmic Ca^{2+}-ATPase (SERCA), thapsigargin (TG, $3\,\mu M$) (41) (Fig. 1D and Supplementary Fig. S2). The increase in $[Ca^{2+}]_{mt}$ observed in response to an elevation in cytosolic Ca^{2+} induced by TG was almost abolished by expression of a dominant-negative pore-forming subunit of MCU (MCUB) (63), confirming the MCU dependence of this mitochondrial Ca^{2+} uptake (Fig. 1D–G). In addition, a significant increase in $[Ca^{2+}]_c$ was detected in cells overexpressing MCUB due to reduced mitochondrial buffering

FIG. 1. **α_1-adrenoceptor (α_1-AR) stimulation accelerates mitochondrial Ca^{2+} uptake in H9c2 cells.** **(A)** Expression of mitochondria-targeted Ca^{2+}-sensitive probe, Mitycam. Mitochondrial location was determined using mt-RFP. A cell stably transfected with only mt-RFP is also shown in the top row to confirm almost no background fluorescence in the GFP channel. Mitycam localized to mitochondria. Scale bars, $20\,\mu$m. **(B)** Color scatter plotting (*right*) and frequency scatter plotting (*left*) obtained from representative pictures in **(A)**. **(C)** Time course of Mitycam fluorescence intensity during $3\,\mu M$ thapsigargin (TG) treatment. Scale bar, $10\,\mu$m. **(D)** *Left*: Representative time courses of $[Ca^{2+}]_{mt}$ (*top*) and $[Ca^{2+}]_c$ (*bottom*) in cells stimulated by TG in control cells (CTR: nontransfected cells) (*black*), MCU (*red*), and MCUB (*blue*)-overexpressed cells. *Arrow* indicates TG application. $[Ca^{2+}]_{mt}$ and $[Ca^{2+}]_c$ were measured using Mitycam and Fura-Red, respectively. Mitycam fluorescence (F) was converted into $1 - (\Delta F/F_0)$, which shows the changes in $[Ca^{2+}]_{mt}$, where F_o stands for initial fluorescence levels. Averaged data are shown in Supplementary Fig. S2. *Right*: summary data of *left panels*. $[Ca^{2+}]_{mt}$ was measured at 60 s after stimulation. For $[Ca^{2+}]_c$, peak $[Ca^{2+}]_c$ within 120 s was measured. *$p < 0.05$, compared to CTR. **(E)** Effect of Phe pretreatment on $[Ca^{2+}]_{mt}$ and $[Ca^{2+}]_c$. Representative time course of $[Ca^{2+}]_{mt}$ (*top*) and $[Ca^{2+}]_c$ (*bottom*) after TG stimulation (*arrow*) in cells with (*red*) or without (*black*) pretreatment with Phe ($100\,\mu M$, 15 min). $[Ca^{2+}]_{mt}$ and $[Ca^{2+}]_c$ were simultaneously measured using Mitycam and Fura-red, respectively, in a single cell (see Supplementary Materials and Methods section). Summary data are shown in Supplementary Fig. S5. **(F)** *Left*: Averaged time course of $[Ca^{2+}]_{mt}$ after TG stimulation (*arrow*) in cells with (*red*) or without (*black*) pretreatment with Phe ($100\,\mu M$, 15 min). $[Ca^{2+}]_{mt}$ in cells overexpressing MCU-DN (blue) or MCUB (sky blue) is also shown for comparison. *Right*: Averaged time course of $[Ca^{2+}]_{mt}$ after TG stimulation (*arrow*) in MCU-transfected cells pretreated with (*red*) or without (*black*) Phe. **(G)** Summary data of **(F)** at 60 s after stimulation. $[Ca^{2+}]_{mt}$ in cell pretreatment with Phe and prazosin (Praz, $1\,\mu M$) (*purple*) is also shown (see also Supplementary Fig. S5). *$p < 0.05$, compared to CTR without Phe treatment. #$p < 0.05$, N.S., not significant. To see this illustration in color, the reader is referred to the web version of this article at www.liebertpub.com/ars

(Fig. 1D and Supplementary Fig. S2). On the other hand, the increase in $[Ca^{2+}]_{mt}$ in response to TG was enhanced and a significant reduction in the $[Ca^{2+}]_c$ in response to TG was observed in MCU overexpressing cells (Fig. 1D–G and Supplementary Fig. S2). This greater mitochondrial response was not secondary to alterations of the cytosolic response, but a rather significant reduction in the $[Ca^{2+}]_c$ transient was observed, due to the increased Ca^{2+} clearance by mitochondria, consistent with previous reports (3, 14, 17).

To test whether α_1-ARS regulates mitochondrial Ca^{2+} uptake, changes in $[Ca^{2+}]_{mt}$ and $[Ca^{2+}]_c$ induced by TG were simultaneously measured in cells pretreated for 15 min with the α_1-AR agonist phenylephrine (Phe, 100 μM). In H9c2 cells, not like other G_q-protein-coupled receptors (G_qPCR) expressed in this cell line (41, 53, 59), acute Phe treatment did

not induce global cytosolic Ca^{2+} elevation indicating a lack of Ca^{2+} release from the sarco/endoplasmic reticulumin (SR/ER) through inositol 1,4,5-trisphosphate (IP₃) receptor (Supplementary Fig. S1), possibly due to the lower endogenous expression levels of α_1-AR and subsequent IP₃ generation upon stimulation (Supplementary Fig. S3) in this cell line. Phe was able to activate downstream signaling equivalent to other G_qPCR agonists (Supplementary Fig. S4). TG induced a higher $[Ca^{2+}]_{mt}$ increase in Phe-pretreated cells compared with untreated cells (Fig. 1E, F). A significant reduction in the $[Ca^{2+}]_c$ transient was also observed, due to the increased Ca^{2+} clearance by mitochondria (Fig. 1E and Supplementary Fig. S5). The increase in $[Ca^{2+}]_{mt}$ observed in Phe-pretreated cells was almost abolished in the presence of the α_1-AR antagonist prazosin (1 μM), confirming that this
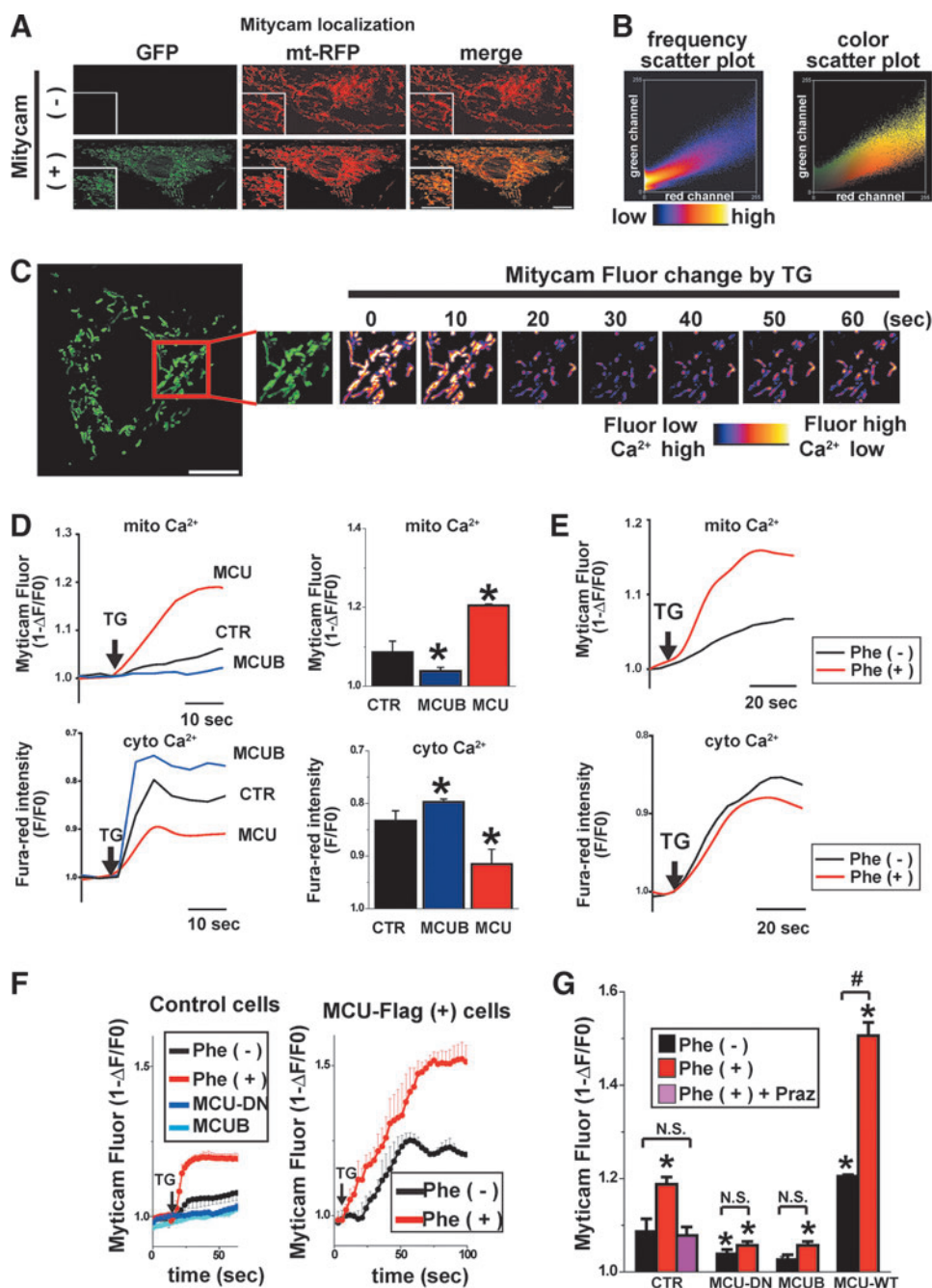
effect is mediated through α_1-ARS (Fig. 1G and Supplementary Fig. S5). Interestingly, peak $[Ca^{2+}]_{mt}$ in Phe-treated cells reached similar levels as that observed in MCU overexpressing cells without Phe pretreatment (Fig. 1F, G).

We also observed the concentration-dependent effect of Phe on $[Ca^{2+}]_{mt}$ elevation. Half maximal effective concentration of Phe was $\cong 2\,\mu M$ (Supplementary Fig. S5). In addition, to test whether β-AR stimulation, which is the major AR isoform in cardiomyocytes, regulates mitochondrial Ca^{2+} uptake, TG-induced $[Ca^{2+}]_{mt}$ changes were measured in cells pretreated for 15 min with the β-AR agonist isoproterenol (Iso, $1\,\mu M$). In Iso-pretreated cells, the increase in $[Ca^{2+}]_{mt}$ was similar to that in nontreated cells, indicating that this effect is specific to α_1-AR signaling (Supplementary Fig. S5). In cells expressing MCUB (63) or a dominant-negative MCU mutant (MCU-DN) (14), TG-induced $[Ca^{2+}]_{mt}$ uptake was significantly reduced and Phe pretreatment did not augment this uptake, demonstrating that Phe stimulation enhances MCU function (Fig. 1F–G). On the other hand, in MCU overexpressing cells, TG-induced $[Ca^{2+}]_{mt}$ uptake reached higher levels following Phe pretreatment (Fig. 1F, G). We also confirmed that in native cultured rat neonatal cardiomyocytes (NCMs), α_1-AR signaling (pretreatment of Phe or a physiological agonist, norepinephrine) can accelerate mitochondrial Ca^{2+} uptake (Supplementary Fig. S6). Thus, α_1-ARS upregulates mitochondrial Ca^{2+} uptake by augmenting MCU function.

α_1-AR stimulation triggers activated Pyk2 translocation from cytosol to mitochondria and MCU tyrosine phosphorylation

The next question is how α_1-ARS can activate MCU function. Our hypothesis is that activated Pyk2 by α_1-ARS phos-

phorylates MCU and accelerates mitochondrial Ca^{2+} uptake. To begin with, we first established a HEK293T cell line stably overexpressing MCU (HEK293T-MCU-Flag cells) to circumvent potential issues related to low endogenous expression of MCU in cultured cells (3, 14) (Fig. 2). We found that a small amount of endogenous Pyk2 was present in mitochondria-enriched fractions and α_1-ARS increased the amount of mitochondrial Pyk2 (named mPyk2) (Fig. 2A). We quantitatively analyzed the ratio of cytosolic and mitochondrial Pyk2 and found that Pyk2 translocated from the cytosol to mitochondria upon Phe stimulation (Fig. 2A). In addition, the amount of activated Pyk2 (autophosphorylated Pyk2) was significantly increased in mitochondria-enriched fraction after α_1-ARS, possibly due to the significant activated Pyk2 translocation from the cytosol to mitochondria (Fig. 2A, B). G_qPCR signaling, including α_1-AR, increases ROS (20) and Pyk2 is known to be activated by ROS (22). Consistent with this mechanism, pretreatment with an antioxidant, N-acetylcysteine or a mitochondria-targeted antioxidant, mito-TEMPO [a specific scavenger of mitochondrial superoxide (mSO)] (73) significantly inhibited α_1-AR-mediated activated Pyk2 translocation from cytosol to mitochondria (Fig. 2A, B and Supplementary Fig. S7). We next used the anti-phosphotyrosine (-P-Tyr) antibody and observed tyrosine phosphorylation of MCU in mitochondria-enriched fraction after Phe stimulation. The intensity of a P-Tyr band identical to the molecular weight of MCU was significantly increased after Phe stimulation, indicating that tyrosine residue(s) in MCU might be phosphorylated after mPyk2 activation (Fig. 2B).

To investigate whether Pyk2 could directly phosphorylate MCU, we determined the submitochondrial localization of Pyk2 using Proteinase K (PK) digestion with a series of detergent concentrations to differentially permeabilize the outer mitochondrial membranes (OMM) and inner mitochondrial
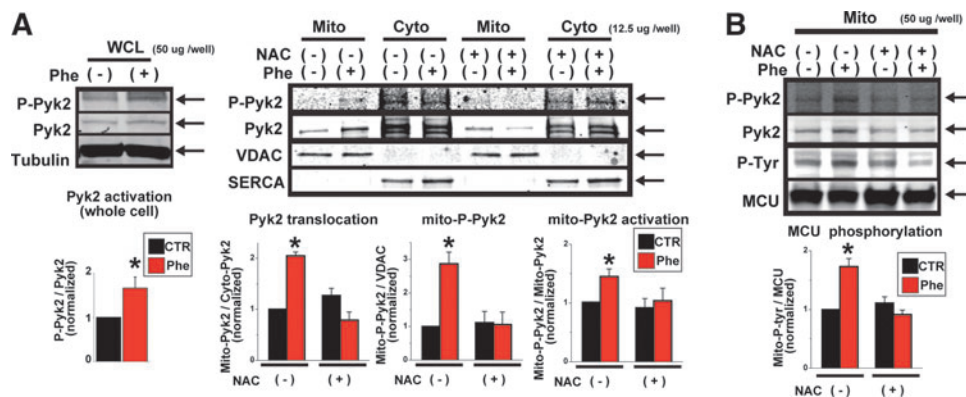

FIG. 2. α_1-AR stimulation induces activated Pyk2 translocation from cytosol in mitochondria and tyrosine phosphorylation of MCU in HEK293T cells. (A) *Right:* Pyk2 activation in HEK293T cells stably overexpressing MCU-Flag after $100\,\mu M$ Phe (15 min), HEK293T cells stably overexpressing MCU-Flag were treated by $100\,\mu M$ Phe for 15 min and whole cell lysates (WCL) were prepared. Proteins were separated by SDS-PAGE ($50\,\mu g$/well). Activated Pyk2 was detected using the anti-phospho-Tyr402-Pyk2 (p-Pyk2) antibody (see Supplementary Materials and Methods section). Summary data are shown at the *bottom.* $*p < 0.05$. *Left:* Pyk2 translocation into mitochondria in HEK293T cells stably overexpressing MCU-Flag after $100\,\mu M$ Phe (15 min). HEK293T cells stably overexpressing MCU-Flag were treated by $100\,\mu M$ Phe for 15 min in the presence of absence of N-acetylcysteine (NAC) and mitochondria-enriched fraction (Mito) and cytosolic fraction (including ER/SR) were prepared. Proteins were separated by SDS-PAGE ($12.5\,\mu g$/well for each fractionated protein). Summary data are shown at the *bottom.* $*p < 0.05$. (B) Pyk2 activation and MCU phosphorylation in mitochondrial fractionation ($50\,\mu g$/well). To increase the signals from P-Pyk2 and Pyk2, $50\,\mu g$ protein of mitochondria-enriched fraction was loaded in each well. MCU phosphorylation was detected by anti-P-Tyr antibody. MCU phosphorylation was estimated by the P-Tyr bands identical to the molecular weight of MCU. $*p < 0.05$. To see this illustration in color, the reader is referred to the web version of this article at www.liebertpub.com/ars

membranes (IMM) (11). Proteins with known localization are immunoblotted and labeled according to their topology (Supplementary Fig. S8). Similar to the matrix protein cyclophilin D (Cyp-D), MCU is resistant to PK proteolysis even under high digitonin concentrations (up to 0.1%), consistent with the idea that MCU termini face to the matrix side. All these proteins, including Cyp-D and MCU, were substrates of PK as evidenced by significant digestion in the presence of Triton X-100. In addition, Pyk2 was also digested only with high digitonin, suggesting that endogenous mPyk2 primarily exists in the matrix and/or is bound to IMM from the matrix side at resting conditions. Interestingly, higher concentrations of digitonin were required to digest Pyk2 after Phe stimulation, suggesting that the amount of matrix mPyk2 increases after Phe stimulation (Supplementary Fig. S8).

Next, we confirmed that Pyk2 could specifically and directly bind to MCU and phosphorylate MCU by *in vitro* binding (72) and kinase assays (37) using purified MCU and Pyk2 proteins (Fig. 3A, B). The MCU-Pyk2 interaction and Pyk2-dependent phosphorylation of MCU were also observed *in situ* by immunoprecipitation (IP) in whole cell lysates (WCL) (Fig. 3C, D) or mitochondrial-enriched protein fractions (Fig. 3E). The MCU-Pyk2 interaction was enhanced after Phe stimulation concomitant with MCU phosphorylation (Fig. 3D, E). The MCU phosphorylation by Phe was inhibited by pretreatment with Mito-TEMPO, confirming that this mechanism is mROS dependent (Supplementary Fig. S7). Moreover, these effects were abolished by expression of a kinase-dead Pyk2 mutant (Pyk2-KD) (Supplementary Fig. S9) or transfection of *si*RNA targeted to Pyk2 (*siRNA-Pyk2*) (Fig. 3F, G).

Together, these results demonstrate that mPyk2 is activated by α_1-AR-dependent and mROS-dependent signaling, which leads to mPyk2 binding to MCU and direct phosphorylation of MCU in the matrix.

Next, we tested whether this α_1-AR-Pyk2-MCU signaling cascade also exists in H9c2 cells. Pyk2 activation, Pyk2 translocation into mitochondria, MCU-Pyk2 interaction, and Pyk2-dependent MCU phosphorylation were detected in this cell line (Fig. 4A–D), similar to those observed in HEK293T cells. We also observed Pyk2 translocation into mitochondria using confocal microscopy under Phe stimulation by cotransfection of GFP-Pyk2 and MCU-DsRed (Fig. 4E). Pyk2 localized in both the cytosol and mitochondria at baseline. After Phe stimulation, a more punctate pattern of GFP-Pyk2 was observed indicating mitochondrial localization. Overlapped coefficient (37, 53) was increased indicating GFP-Pyk2 translocation into mitochondria and colocalization with MCU-RFP after Phe stimulation (Fig. 4E). We also performed Förster resonance energy transfer (FRET) analysis by imaging the combination of GFP-Pyk2 (donor) and MCU-DsRed (acceptor) to determine the interaction of these two molecules *in situ* (Fig. 4F, G). The FRET signal from GFP-Pyk2/MCU-Dsred at rest was higher than that observed from the cells coexpressing GFP and MCU-Dsred, suggesting that there is a specific interaction of Pyk2 and MCU *in situ* (Fig. 4F). After Phe stimulation, the FRET signal from GFP-Pyk2/MCU-Dsred increased in a time-dependent manner (Fig. 4G). These data demonstrate that α_1-ARS triggers activated Pyk2 translocation from cytosol to mitochondria, where it interacts with MCU and phosphorylates MCU in H9c2 cells.

We next asked whether this signaling also occurs in native cardiomyocytes. In native cardiomyocytes, a high dose of Phe ($>10\,\mu M$) shows less receptor specificity and activates not only α_1-AR signaling but also nonselectively activates β-AR signaling due to the high expression level of β-AR (58). Therefore, we used a β-AR antagonist, $1\,\mu M$ propranolol in the extracellular solution for stimulation of native cardiomyocytes with Phe to block the contamination of β-AR effects (58). In NCMs, activated Pyk2 was translocated from cytosol to mitochondria and phosphorylated MCU during Phe (Fig. 5A–C). In isolated rat adult cardiomyocytes (ACMs), Pyk2 was also activated and phosphorylates MCU upon α_1-ARS (Fig. 5D, E). These effects in NCMs and ACMs were abolished by pretreatment of α_1-AR antagonist, prazosin, or focal adhesion kinase (FAK)/Pyk2 selective inhibitor, PF-431396 (Fig. 5). Collectively, Pyk2 is activated by α_1-ARS, imported into mitochondria and directly phosphorylates MCU in native cardiomyocytes.

α_1-AR-Pyk2 signaling regulates MCU channel oligomerization and function

We next addressed the mechanism by which Pyk2-dependent MCU phosphorylation activates MCU-dependent mitochondrial Ca^{2+} uptake. A single MCU protein contains two transmembrane domains and MCU needs to be oligomerized to form channels (14, 63). Therefore, our next hypothesis is that Pyk2-dependent MCU phosphorylation enhances MCU oligomerization (*i.e.*, channel pore formation). At first, MCU-GFP was transfected into HEK293T-MCU-Flag cells (Supplementary Fig. S10). After Phe stimulation, binding of MCU-GFP and MCU-Flag was significantly increased after Phe stimulation, suggesting that interaction of MCU monomers with different tags was enhanced by α_1-ARS *in situ* to form a higher order complex (Supplementary Fig. S10). Next, we performed conventional native gel separation of whole cell lysates from HEK293T-MCU-Flag cells and found that MCU migrated at a molecular weight of $\sim140\,kDa$ (Fig. 6). The size of the MCU monomer and oligomer observed here was consistent with our observation using wheat germ lysates expressing MCU (63). The magnitude of this higher order complex increased following 15 min of Phe stimulation, which was blocked by either Mito-TEMPO or Pyk2-knockdown (Fig. 6B, C). Similar results were obtained using mitochondria-enriched fractionation proteins (Supplementary Fig. S11). These results indicate that α_1-AR-Pyk2-dependent MCU phosphorylation promotes MCU oligomerization.

Finally, we tested whether Pyk2 activation during α_1-AR enhances mitochondrial Ca^{2+} uptake in H9c2 cells using the protocol shown in Figure 1. Pyk2 is known as a Ca^{2+}- and ROS-dependent kinase, but 10 min of TG treatment did not activate Pyk2 in this cell line, confirming that our protocol for triggering mitochondrial Ca^{2+} accumulation itself did not significantly activate Pyk2 through increased $[Ca^{2+}]_c$ (Supplementary Fig. S12). The increase in $[Ca^{2+}]_{mt}$ observed in Phe-pretreated cells was abolished in the presence of PF-431396, indicating that this effect is mediated by Pyk2 or FAK activity (Fig. 7A, right). The treatment with PF-431396 itself did not change the peak $[Ca^{2+}]_c$ (Fig. 7A, left). Next, we transfected the plasmid containing *siRNA-Pyk2* (67) into H9c2 cells (Fig. 7B and Supplementary Fig. S13). The increase in $[Ca^{2+}]_{mt}$ observed in Phe-pretreated cells was abolished in the cells transfected by *siRNA-Pyk2*, indicating
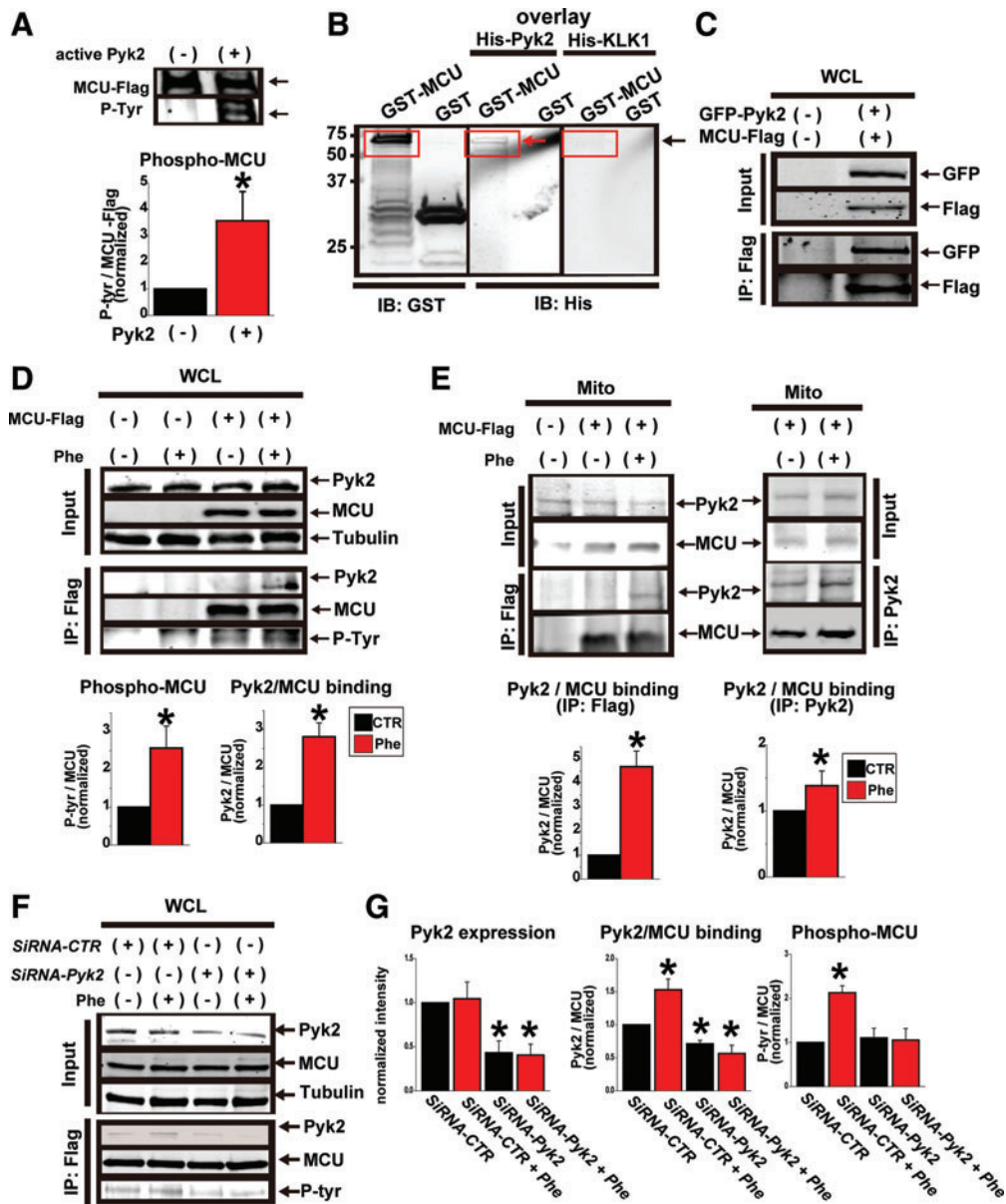
FIG. 3. Pyk2 binds to MCU and directly phosphorylates MCU. (A) *In vitro* kinase assay. *Top:* MCU-flag produced in HEK293T cells stably overexpressing MCU-Flag was collected by IP and treated with Pyk2 kinase-domain peptide (active Pyk2) (see Supplementary Materials and Methods section). *Bottom:* Summary data of MCU phosphorylation. *$p < 0.05$. **(B)** Protein membrane overlay (*in vitro* binding) assay using GST-MCU and His-Pyk2 (see Supplementary Materials and Methods section). His-Pyk2 specifically bound to GST-MCU (*red*) after overlay (*middle panel*), but His-kallikrein-1 (KLK-1) (serine protease) did not (*right panel*). (see Supplementary Materials and Methods section). **(C)** *In situ* binding assay in HEK293T cells transected with GFP-Pyk2 and MCU-flag. **(D)** *In situ* binding assay in HEK293T cells stably overexpressing MCU-Flag. *Top*: IP was performed using. WCL before and after Phe stimulation. MCU phosphorylation was detected by anti-P-Tyr antibody. Phosphorylation of MCU and interaction of MCU and Pyk2 significantly increased after Phe stimulation. *Bottom*: Summary data of MCU phosphorylation and MCU/Pyk2 binding. *$p < 0.05$. **(E)** IP of mitochondria fraction by anti-Flag (*left*) or anti-Pyk2 (*right*) antibodies. Nontransfected cells were used as control. *$p < 0.05$. **(F)** *In situ* binding assay in HEK293T cells stably overexpressing MCU-Flag with or without Pyk2 knock down by *siRNA-Pyk2*. IP was performed by anti-Flag antibody using WCL before and after Phe stimulation with or without Pyk2 knock down. **(G)** Summary data of **(F)**. To see this illustration in color, the reader is referred to the web version of this article at www.liebertpub.com/ars

that Pyk2 is necessary for this effect (Fig. 7B). Collectively, these results show that α_1-AR-Pyk2-dependent MCU tyrosine phosphorylation promotes MCU oligomerization, leading to the facilitation of mitochondrial Ca^{2+} uptake through MCU.

α_1-AR-Pyk2 signaling triggers MCU-dependent ROS generation and proapoptotic protein release

Excessive mitochondrial Ca^{2+} uptake increases ROS production from mitochondria in cardiomyocytes (31). In

FIG. 4. **α_1-AR stimulation activates Pyk2 and phosphorylates MCU in H9c2 cells.** **(A)** *Top*: Time-dependent activation of Pyk2 in WCL during application of 100 μM Phe. *Bottom*: Summary data of *top panel*. *$p < 0.05$ compared to nontreated cells (0 min). **(B)** *Top*: Pyk2 translocation from cytosol to mitochondria by Phe stimulation (100 μM, 15 min). *Bottom*: Summary data of top panels. *$p < 0.05$ compared to nontreated cells. **(C)** *Left:* IP of WCL by anti-MCU antibody. *Right:* Quantitative analysis of MCU phosphorylation after Phe stimulation obtained from *left panel*. **(D)** *Left*: IP of mitochondrial fractions by anti-MCU antibody. *Right:* Quantitative analysis of MCU phosphorylation after Phe stimulation obtained from *left panel*. **(E)** *Left*: Time-dependent GFP-Pyk2 translocation by Phe stimulation (100 μM, 30 min) in a single cell. *Right*: Summary data of overlapped coefficient analysis before and after Phe stimulation (see also Supplementary Materials and Methods section). *$p < 0.05$. **(F)** Comparisons of FRET efficiency between the cells expressing GFP-Pyk2/MCU-DsRed and GFP/MCU-DsRed. FRET efficiency was significantly higher in cells expressing GFP-Pyk2/MCU–DsRed. The ratio of the emission intensity at 583 nm (DsRed) to 508 nm (GFP) represented FRET efficiency (see Supplementary Materials and Methods section). *$p < 0.05$. **(G)** Time-dependent changes in FRET efficiency after Phe stimulation (100 μM, 30 min) in cells expressing GFP-Pyk2 and MCU-DsRed (see Supplementary Materials and Methods section). Cells stimulated by vehicle (water) are shown as control. To see this illustration in color, the reader is referred to the web version of this article at www.liebertpub.com/ars

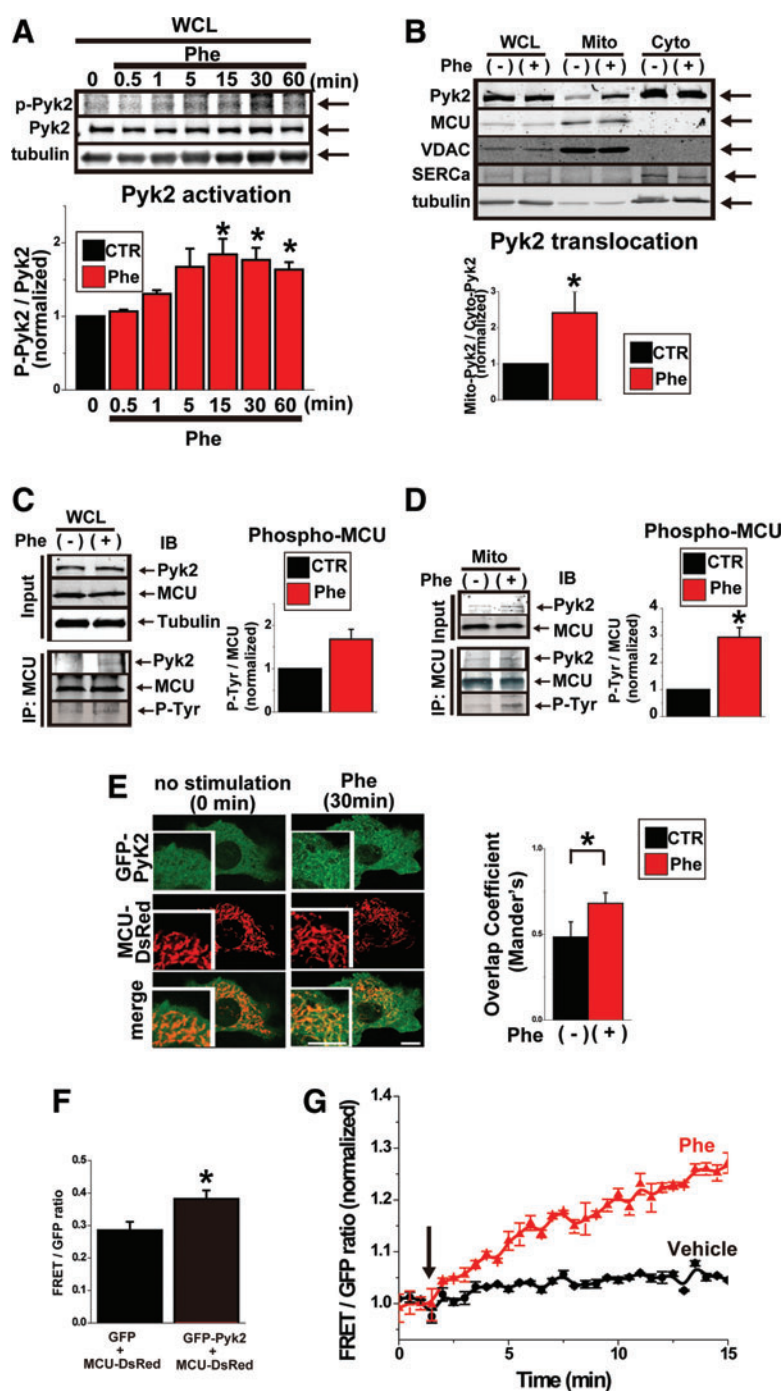addition, mitochondrial Ca^{2+} overload results in mitochondrial membrane potential ($\Delta\Psi_m$) depolarization, ROS overproduction, and release of the proapoptotic proteins into the cytosol, ultimately resulting in cell injury and death. Our data clearly showed that α_1-AR-Pyk2 signaling strongly elevates [Ca^{2+}]$_{mt}$ (Figs. 1–7) and that this increase is maintained at higher levels after α_1-ARS. This sustained increase in mitochondrial Ca^{2+} could significantly enhance mROS production and apoptotic signals. Therefore, we tested whether α_1-ARS increases the mitochondrial levels of ROS in H9c2 cells using the mSO indicator MitoSOX-Red (53) (Fig. 8). Basal MitoSOX-Red intensity was significantly decreased by Mito-TEMPO pretreatment, confirming that MitoSOX-Red

is sensitive to mSO (Fig. 8B). We found that Phe treatment significantly increased mSO levels and this effect was abolished by the pretreatment of Mito-TEMPO (Fig. 8A, B). Next, cells were pretreated by a potent FAK/Pyk2 inhibitor PF-431396. Pretreatment of PF-431396 dramatically blocked Phe-induced ROS increase (Fig. 8B). Moreover, we used the cells transfected with *siRNA-Pyk2* (Supplementary Fig. S13). Basal MitoSOX-Red intensity in cells transfected by *siRNA-Pyk2* was significantly lower than that in cells treated with control vector, indicating that Pyk2 is involved in the maintenance of basal mSO levels (Fig. 8B). Pyk2 knockdown significantly blocked the Phe-induced increase in MitoSOX-Red intensity, confirming that the increase in mSO levels by
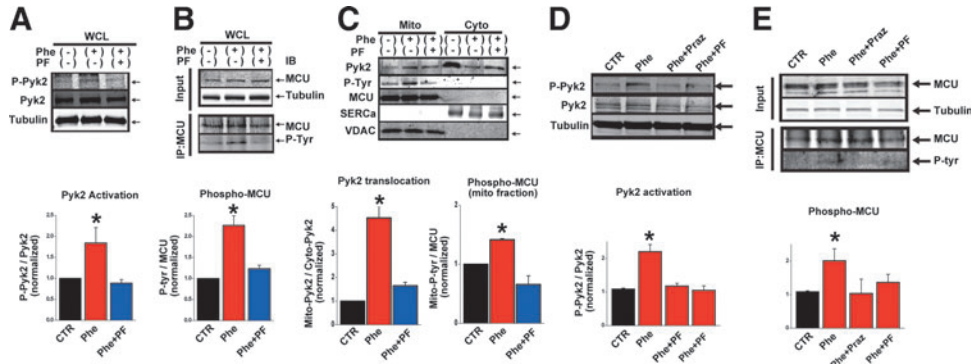
FIG. 5. α₁-AR stimulation activates Pyk2 and phosphorylates MCU in native cardiomyocytes. (A) Neonatal cardiomyocytes (NCMs) were treated by 100 μM Phe (in the presence of 1 μM propranolol) for 15 min with or without Pyk2 inhibitor (PF) and WCL were prepared. *$p < 0.05$ compared to the cells without stimulation (*black*). (B) Detection of MCU tyrosine phosphorylation after IP by anti-MCU antibody using WCL. MCU phosphorylation was detected by anti-P-Tyr antibody. $p < 0.05$ compared to the cells without stimulation (*black*). (C) *Top:* Pyk2 translocation and MCU phosphorylation after Phe stimulation in NCMs. *Bottom:* Summary data. *$p < 0.05$ compared to the cells without stimulation (*black*). (D) *Top:* Isolated adult cardiomyocytes (ACMs) were treated by 100 μM Phe (in the presence of 1 μM propranolol) for 30 min with or without α₁-AR antagonist prazosin (Praz) or Pyk2 inhibitor (PF) and WCL were prepared. *Bottom*: Summary data. *$p < 0.05$. (E) Detection of MCU tyrosine phosphorylation after IP by anti-MCU antibody using WCL. $p < 0.05$ compared to the cells without stimulation (*black*). To see this illustration in color, the reader is referred to the web version of this article at www.liebertpub.com/ars

Phe was mediated through α₁-AR-Pyk2 signaling. In addition, in cells overexpressing MCUB, MitoSOX-Red intensity in basal conditions significantly decreased compared with those in control cells and the Phe-induced increase in Mito-SOX-Red intensity was completely abolished (Fig. 8B).

These results indicate that Phe stimulates mSO levels *via* α₁-AR-Pyk2-MCU signaling.

Because high levels of mROS trigger the release of mitochondrial intermembrane space proteins to the cytosol to initiate apoptosis through increasing the OMM permeability
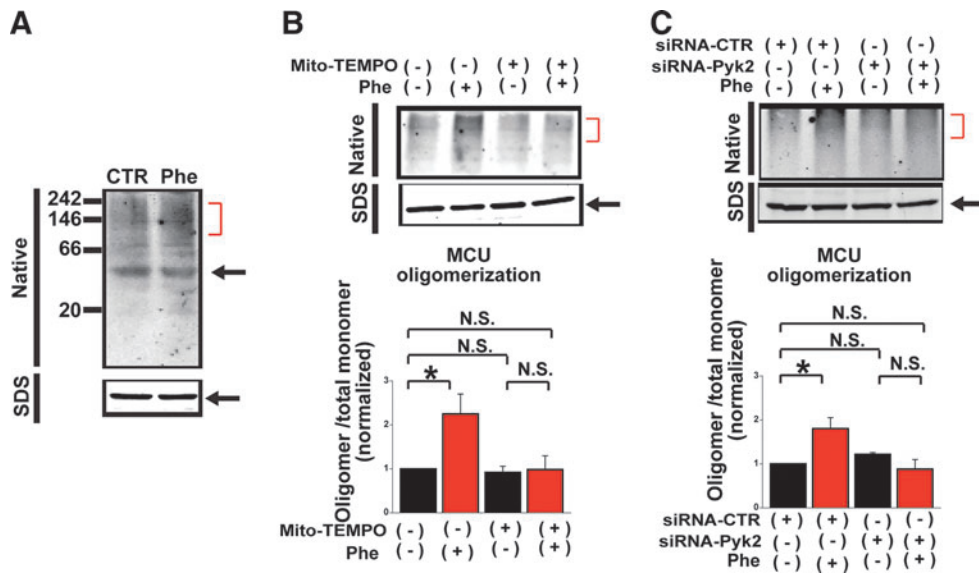

FIG. 6. α₁-AR stimulation enhances the oligomerization of MCU *via* Pyk2 activation. (A) Representative Native PAGE of WCL from HEK293T cells stably overexpressing MCU-Flag treated by Phe. Membranes were blotted with anti-Flag antibody. MCU monomer bands in Native PAGE and SDS PAGE are shown with an arrow. MCU monomer bands in SDS PAGE are shown as loading control. A higher band ~140 kDa (smear distribution shown as a *red square bracket*), which is compatible with a tetramer, indicating that MCU monomers were oligomerized in higher order complexes *in situ*. (B) Mito-TEMPO pretreatment inhibits Phe-induced MCU oligomerization. MCU oligomerization (within a *red square bracket*) was quantified by normalizing with MCU monomer in SDS-PAGE (*bottom*). *$p < 0.05$. N.S., not significant. (C) Pyk2 knockdown inhibits Phe-induced MCU oligomerization (see also Fig. 3F, G). MCU oligomerization (within a *red square bracket*) was quantified by normalizing with MCU monomer in SDS-PAGE (*bottom*). *$p < 0.05$. N.S., not significant. To see this illustration in color, the reader is referred to the web version of this article at www.liebertpub.com/ars

FIG. 7. α_1-AR-Pyk2 signaling accelerates mitochondrial Ca^{2+} uptake. (A) Effect of Phe pretreatment on [Ca^{2+}]$_{mt}$ and [Ca^{2+}]$_c$ in the presence or absence of FAK/Pyk2 inhibitor (PF). [Ca^{2+}]$_{mt}$ (*right*) and [Ca^{2+}]$_c$ (*left*) after TG stimulation in cells with or without pretreatment of Phe and PF are shown. PF was applied before Phe stimulation (2 h before Phe application). [Ca^{2+}]$_{mt}$ and [Ca^{2+}]$_c$ were measured using Mitycam and Fura-red, respectively (see Supplementary Materials and Methods section). *$p < 0.05$. **(B)** Effect of Phe pretreatment on [Ca^{2+}]$_{mt}$ and [Ca^{2+}]$_c$ in Pyk2-knockdown H9c2 cells. Knockdown efficiency is shown in Supplementary Fig. S13. [Ca^{2+}]$_{mt}$ (*right*) and [Ca^{2+}]$_c$ (*left*) after TG stimulation in cells with or without transfection of a plasmid containing *siRNA-Pyk2* are shown. *$p < 0.05$. To see this illustration in color, the reader is referred to the web version of this article at www.liebertpub.com/ars
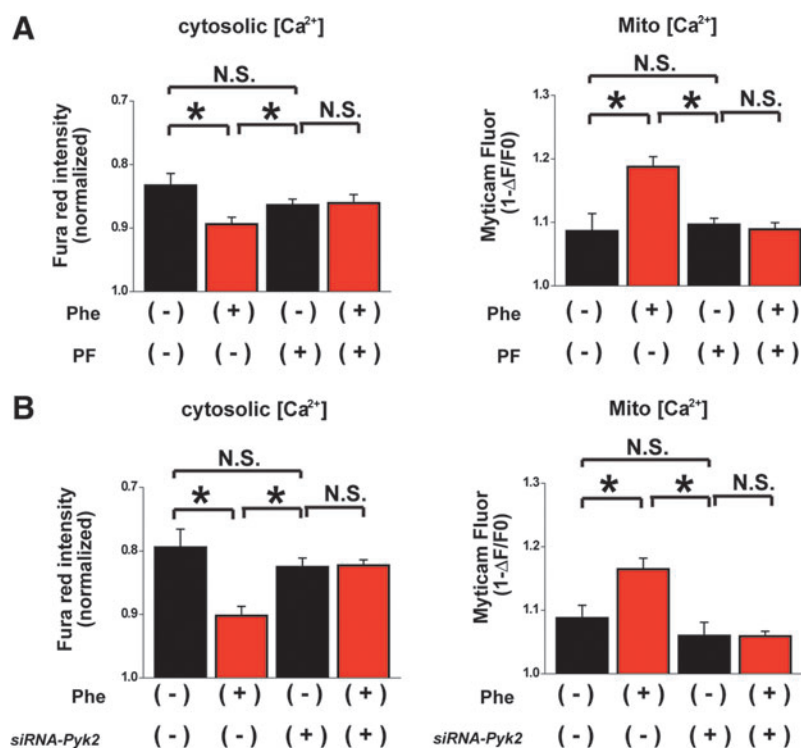
(*e.g.*, by mPTP opening) (75), we determined whether α_1-ARS promotes proapoptotic protein release. We used a fluorescence-tagged mitochondrial intermembrane space protein, GFP-tagged second mitochondrial-derived activator of caspase (Smac) to follow the time-dependent release of proapoptotic proteins during α_1-ARS (Fig. 8C–E) (49). We analyzed changes in pixel intensity standard deviation (punctate/diffuse index) as an index of Smac-GFP release from mitochondria (49). The mitochondrial uncoupler carbonyl cyanide 4-(trifluoromethoxy)phenylhydrazone (FCCP) was used as a positive control to depolarize $\Delta\Psi_m$ to trigger mPTP opening (15). After FCCP treatment, Smac-GFP release into the cytosol (monitored by the decrease in punctate/diffuse index) was within 5 min (Fig. 8C, D). Over 15–20 min of continuous stimulation, high-dose Phe releases a small amount of Smac-GFP into the cytosol (Fig. 8C–E). Phe-induced Smac-GFP release was completely blocked by either the α_1-AR antagonist prazosin, overexpression of MCU-DN, or addition of PF-431396 (2, 65) (Fig. 8D, E). In addition, the Phe-induced proapoptotic protein release was confirmed by detecting cytochrome C in enriched cytosolic and mitochondrial fractions (Fig. 8F). Furthermore, significant activation of caspase 3 was observed following prolonged Phe stimulation, consistent with the idea that α_1-ARS initiated destructive apoptotic cascades following proapoptotic protein release (Fig. 8G). The results from Figure 8 indicate that Phe stimulation induces activation of apoptotic signaling cascades through the α_1-AR-Pyk2-MCU-ROS signaling cascade in H9c2 cells.

α_1-AR-Pyk2 signaling triggers mSO generation and cell death in native cardiomyocytes

We next determined whether this cell death signaling through the α_1-AR-Pyk2-MCU-mROS cascade occurs in ACMs. We used mitochondria-targeted circularly permuted YFP (mt-

cpYFP) to monitor mSO before and after Phe stimulation. This biosensor was recently reported from our groups, which can detect a stochastic and transient superoxide burst from either single or restricted clusters of interconnected mitochondria or isolated mitochondria (termed as a ''mitochondrial superoxide flash'' (mSOF)) (73). The mSOF generation is a result of a small increase in constitutive ROS production in mitochondria, which transiently opens a large channel of mPTP to evoke transient $\Delta\Psi_m$ depolarization, and subsequently stimulates the ETC to produce a burst in O$_2^-$ production. Using this biosensor, we found that Phe significantly increased the frequency of mSOF in ACMs (Fig. 9A, B). Pretreatment with prazosin or PF-431396 inhibited the increase of mSOF induced by Phe, indicating that the Phe-induced mSO generation is mediated through the α_1-AR-Pyk2 signaling pathway (Fig. 9A, B).

Furthermore, we examined whether α_1-AR-Pyk2-mROS signaling initiates destructive apoptotic cascades in ACMs. Significant caspase 3 activation was observed after 30 min of Phe stimulation, consistent with the results observed in H9c2 cells (Fig. 9C), but 30 min of Phe stimulation did not increase cardiomyocyte death (data not shown). Next, we observed the ACM viability after Phe stimulation up to 24 h of treatment by cell morphology (counting the number of rod-shaped cells) under a light microscope (Fig. 9D and Supplementary Fig. S14). We found that over 6 h of Phe stimulation significantly increased ACM death. Conversely, pretreatment with prazosin or PF-431396 inhibited the increase of cell death induced by Phe. We also found that ACMs with abnormal morphology after Phe treatment had a higher activity of caspase-3/7, confirming that this Phe-induced cell death is mediated *via* the apoptotic cascade (Fig. 9E, F). The pretreatment of prazosin, PF-431396, or mito-TEMPO attenuated cell apoptosis induced by 6 h of Phe treatment. These data indicate that the α_1-AR-Pyk2 signaling pathway induces cell death in ACMs possibly through an increase in mSO.
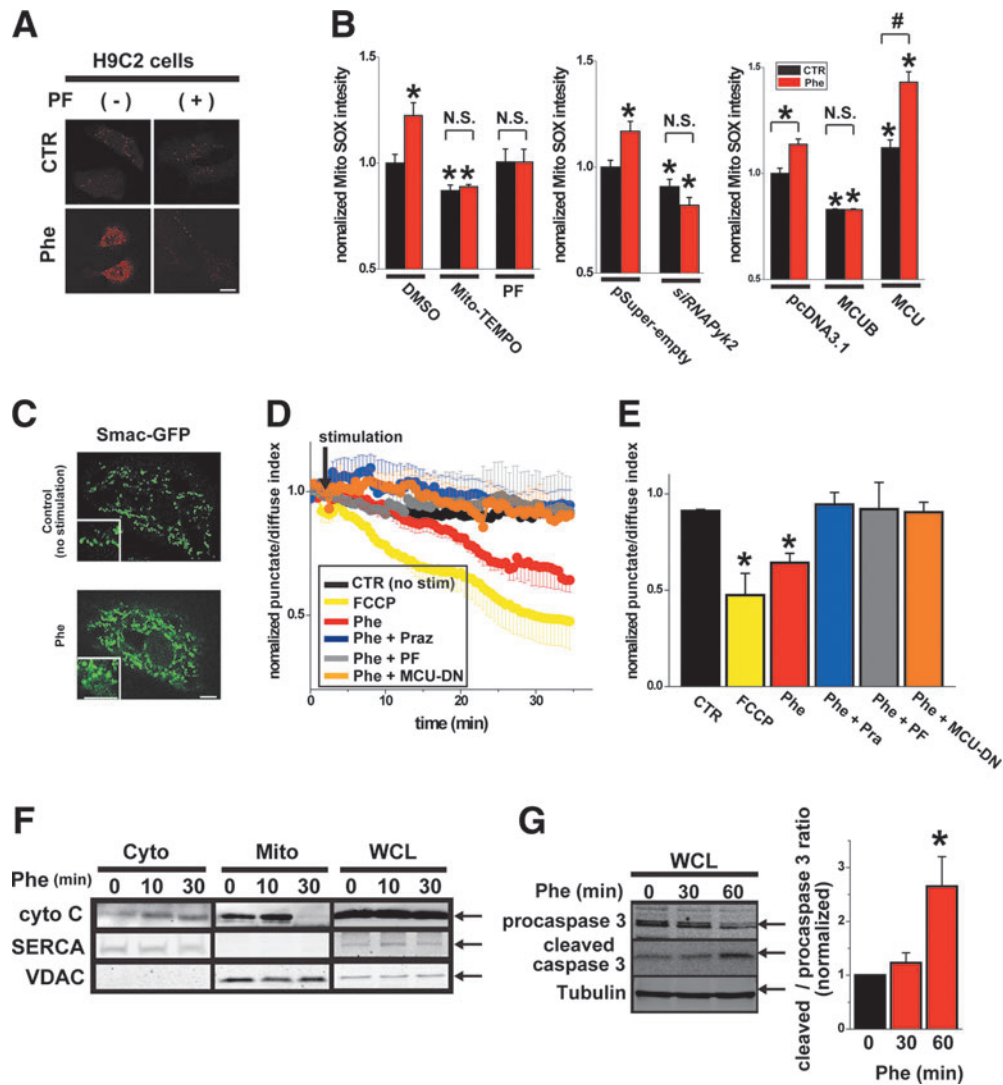
FIG. 8. **α₁-AR-Pyk2-MCU signaling increases mROS levels and initiates apoptotic signaling in H9c2 cells.** **(A)** Mitochondrial superoxide (mSO) levels induced before and after Phe stimulation (30 min, 100 μM) in H9C2 cells measured by MitoSOX-Red in the presence or absence of Pyk2 inhibitor PF-431396 (PF). Scale bar, 20 μm. **(B)** *Left*: PF or Mito-TEMPO pretreatment prevented Phe-induced increases in mSO level. *$p < 0.05$, compared to the control cells treated with DMSO (vehicle) before Phe stimulation. *Middle*: Pyk2 knockdown prevented Phe-induced increases in mSO level. *$p < 0.05$, compared to the control cells transfected with control siRNA vector. *Right*: Overexpression of MCUB prevented Phe-induced increases in mSO level, whereas overexpression of MCU enhanced this effect. *$p < 0.05$, compared to the control cells transfected with pcDNA3.1 empty vector before Phe stimulation. #$p < 0.05$. N.S., not significant. **(C)** Subcellular localization of Smac-GFP before and after Phe stimulation (100 μM, 30 min). Scale bars, 10 μm. **(D)** Time dependence of outer mitochondrial membrane (OMM) permeabilization by Phe using Smac-GFP punctate/diffuse index in the presence or absence of prazosin (Praz), PF-431396 (PF), or MCU-DN overexpression (MCU-DN). FCCP-treated cells are shown as a positive control *(yellow)*. **(E)** Summary data of **(D)** at 35 min. *$p < 0.05$ compared to control cells (nontreated cells). **(F)** Time-dependent cytochrome C release from mitochondria to cytosol by α₁-AR stimulation. Cells were stimulated with 100 μM Phe and cytosolic and mitochondria-enriched fractionations were prepared. WCL were also blotted to show the total amount of cytochrome C *(right panel)*. SERCA2 and VDAC were used to confirm the purity of the cytosolic (including SR/ER) and mitochondrial fractions, respectively. The blots shown are representative of 3 replicates. **(G)** *Left:* Time-dependent caspase 3 activation by α₁-AR signaling. Cells were stimulated by 100 μM Phe for 30 min or 60 min and WCL were prepared to detect procaspase 3 and cleaved caspase 3. Caspase 3 activity was evaluated by the cleaved caspase 3/procaspase 3 ratio. *Right:* Summary data. $p < 0.05$ compared to nontreated cells (0 min). To see this illustration in color, the reader is referred to the web version of this article at www.liebertpub.com/ars

Discussion

In this study, we identified a signaling pathway that regulates mitochondrial Ca²⁺ uptake, ROS production, and apoptotic signaling through a posttranslational modification of MCU (Fig. 10). Specifically, we found that Pyk2 activated downstream of α₁-ARS, translocates into the mitochondria matrix, where it directly phosphorylates MCU tyrosine residue(s), which leads to an increase in the number of functional tetrameric MCU channels by promoting MCU oligomerization.
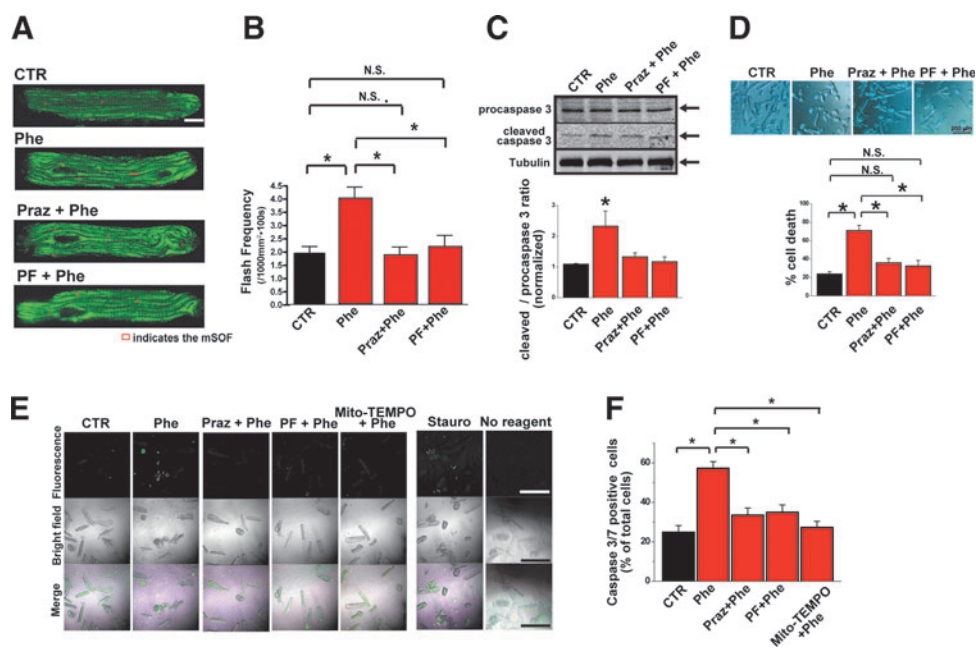
FIG. 9. **α$_1$-AR-Pyk2 signaling accelerates mSO generation and initiates cell death in adult cardiomyocytes.** **(A)** Representative images of mSO flashes (mSOF) observed in ACMs after Phe stimulation (10 min, 100 μM with 1 μM propranolol) by using mitochondrial-targeted cpYFP (see Supplementary Materials and Methods section). **(B)** Summary data of mSOF frequency. Pretreatment of prazosin (Praz) (30 min, 1 μM) or PF-431396 (PF) (2 h, 10 μM) efficiently inhibits the increase of mSOF induced by Phe. mSOF were collected from 18 cells isolated from three rats. *$p < 0.05$. Scale bar, 10 μm. **(C)** *Top*: Caspase 3 activation by α$_1$-AR signaling. Cells were stimulated by Phe for 30 min and WCL were prepared to detect procaspase 3 and cleaved caspase 3. Caspase 3 activity was evaluated by the cleaved caspase 3/procaspase 3 ratio. *Bottom*: Summary data. **(D)** *Top*: Six-hour treatment with Phe increased ACM death. Cell variability was monitored by cardiomyocyte morphology. Pretreatment of Praz or PF efficiently inhibits the increase in cell death induced by Phe. *Bottom*: Summary data. *$p < 0.05$. **(E)** Phe induces apoptosis in primary cultured cardiomyocytes. The pretreatment of Praz (30 min, 1 μM), PF (2 h, 10 μM), or Mito-TEMPO (1 h, 1 μM) attenuated cell apoptosis induced by 6-h Phe treatment. Apoptosis was detected by confocal (exitation/emission:488 nm/525 nm) in live cells after staining with a fluorogenic substrate for activated caspase-3/7 (CellEvent™ Caspase-3/7 Green Detection Reagent) (see also Supplementary Materials and Methods section). Cell morphology was also observed under brightfield. As a positive control, cells were treated by staurosporine (Stauro, 1 μM, 6 h). Images obtained from cells without staining with the detection reagent were also shown as a negative control. Scale bars, 200 μm. **(F)** Summary data of **(E)**. Images were randomly collected from 11–14 image fields from two rats. *$p < 0.05$. To see this illustration in color, the reader is referred to the web version of this article at www.liebertpub.com/ars

Moreover, this α$_1$-AR-Pyk2-MCU signaling cascade enhances mitochondrial Ca^{2+} uptake, mSO generation, and proapoptotic protein release, which initiates the apoptotic cascade and finally leads to cardiomyocyte death (Fig. 9). These results provide new insights into the molecular basis of adrenergic modulation of mitochondrial Ca^{2+} handling and apoptosis. Furthermore, the results of this study unveil a new pathway that could be targeted for the development of novel drugs to protect against the pathophysiological conditions, where increased α$_1$-ARS (36) and mitochondrial injury (25) are known to coexist.

Molecular mechanism underlying enhanced mitochondrial Ca^{2+} uptake by α$_1$-AR-Pyk2-dependent phosphorylation of MCU

We showed here that Pyk2 activation during α$_1$-ARS increases mitochondrial Ca^{2+} uptake through tyrosine phosphorylation of MCU, which enhances MCU oligomerization. This evidence strongly supports the hypothesis that Pyk2-mediated MCU oligomerization is directly linked to an increase in mitochondrial Ca^{2+} uptake following α$_1$-ARS. We

also confirmed the MCU topology at IMM and detailed mPyk2 submitochondrial localization: (i) MCU termini are located at the matrix side as reported (9, 11, 46), (ii) mPyk2 is predominantly localized in the matrix, and (iii) Phe stimulation induces Pyk2 translocation from the cytosol to matrix. This observation suggests that Pyk2 can interact with MCU from the matrix side and directly phosphorylate the channel on either the N- or C-termini, which are known to be important for channel function (12). Recent broad screening of Pyk2-specific substrates using phosphoproteomics to identify consensus substrate motifs for Pyk2 has not yet been established (6). Human MCU contains 15 tyrosine residues; 5 in the N-terminus and 6 in the C-terminus, which are conserved across all eukaryotic species. No tyrosine residues are located in the pore-forming region (14). However, only three of these tyrosine residues (Y158 at N-terminus, Y289, and Y317 at C-terminus) are predicted to be potential PTK phosphorylation sites using the NetPhos 2.0 phosphorylation prediction program (5) and only one of these sites (Y289) is predicted to be a potential FAK/Pyk2-specific phosphorylation site using the Group-based Prediction System (74). Interestingly, basal
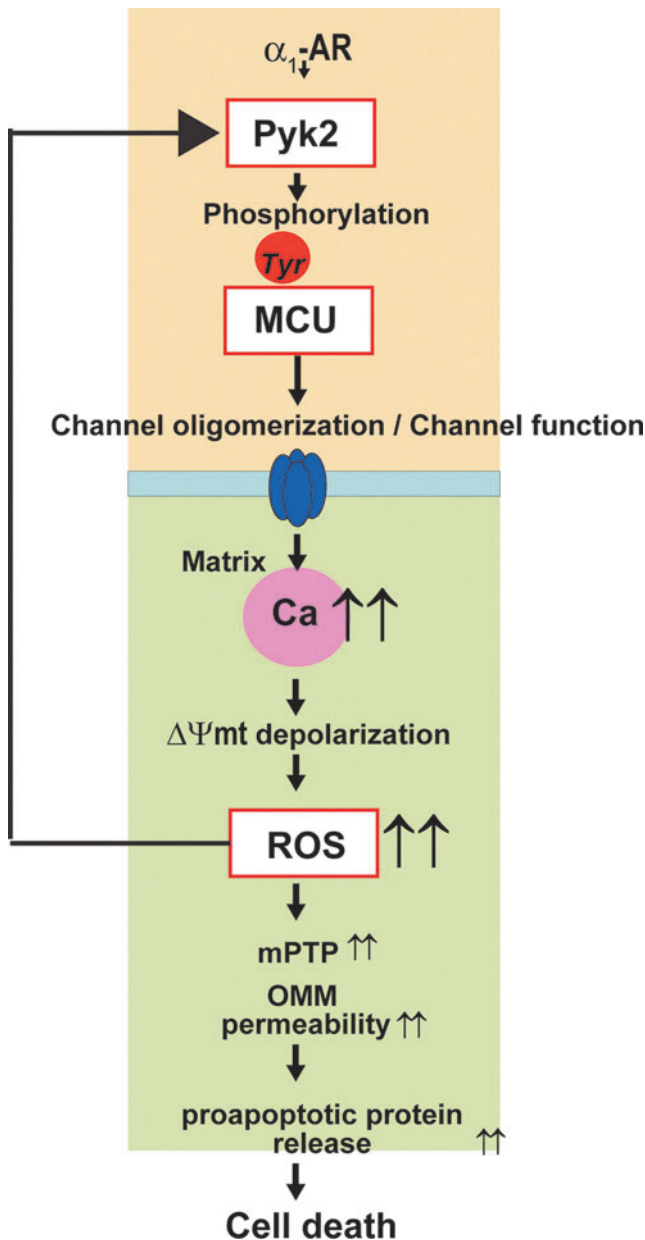
FIG. 10. Working model: Cardiac α_1-AR-Pyk2-dependent MCU phosphorylation initiates mitochondrial Ca^{2+} entry, mSO generation, and cell death. To see this illustration in color, the reader is referred to the web version of this article at www.liebertpub.com/ars

Y289 phosphorylation was reported following mass spectroscopy of human tissue (PhosphoSite) (32, 33). Future studies are needed to definitively determine Pyk2-specific phosphorylation site(s) in MCU and to test the functional importance of these sites using nonphosphorylation and phosphorylation mimetic MCU mutants. In addition, since the basal tyrosine phosphorylation of MCU was not completely abolished by Mito-TEMPO or *siRNA-Pyk2* application (Fig. 3 and Supplementary Fig. S7), suggesting that not only Pyk2 but also other PTK in the mitochondrial matrix (*e.g.*, Src) might regulate the basal tyrosine phosphorylation level of MCU *in situ* (28). Two potential CaMKII phos-

phorylation motifs in the N-terminus of MCU were identified using a nonphosphomutagenesis approach and mutation of these sites abolishes CaMKII-dependent activation of MCU current in mitoplast patch-clamp experiments (38). In this study, we also tested the effect of β-AR signaling on $[Ca^{2+}]_{mt}$, which can activate a variety of serine/threonine kinase, including CaMKII, but this signaling did not significantly alter TG-induced $[Ca^{2+}]_{mt}$ elevation in H9c2 cells (Supplementary Fig. S5C). The amount of mitochondrial Ca^{2+} uptake is generally regulated by the magnitude of $[Ca^{2+}]_c$ elevation in all cell types (56). Therefore, it is a reasonable idea that β-AR signaling has a more prominent effect on the amount of mitochondrial Ca^{2+} uptake due to its strong modulation of the cytosolic Ca^{2+} transient (CaT) size compared to α_1-AR signaling in ACMs. Our observation of α_1-AR-Pyk2-dependent MCU phosphorylation and its channel activation may serve as a supportive or additional mechanism for accelerating mitochondrial Ca^{2+} in response to the enhanced CaT under the physiological adrenergic stimulation. In addition, α_1-AR might play more significant roles when β-AR signaling is downregulated, such as during heart failure. Future study will address the role of α_1-AR-Pyk2-MCU signaling during beat-to-beat CaT and/or in the presence of main adrenergic signaling, β-AR stimulation in ACMs.

Our results also do not rule out the possibility that α_1-AR-Pyk2-dependent tyrosine phosphorylation of MCU alters regulation of MCU by its auxiliary proteins (*e.g.*, MICU1) (11), which may change its Ca^{2+} sensitivity and enhance the mitochondrial Ca^{2+} uptake rate. Indeed, Phe is capable of increasing both mROS production and OMM permeability in the absence of TG-induced global Ca^{2+} elevation (Figs. 8 and 9). These data suggest that there might be another mechanism for the enhancement of the mitochondrial Ca^{2+} clearance by α_1-AR-Pyk2 signaling in addition to the MCU oligomerization. In cardiac cells, α_1-ARS increases the resting (diastolic) $[Ca^{2+}]_c$ levels (34, 44, 61) and/or spontaneous Ca^{2+} release (45) although its effect to peak $[Ca^{2+}]_c$ is relatively small. Therefore, after 15 min of Phe stimulation, α_1-AR-AR-Pyk2 signaling may change the Ca^{2+} sensitivity of MCU through channel tyrosine phosphorylation and mitochondria might accumulate Ca^{2+} more efficiently under the enhancement of spontaneous Ca^{2+} releases from ER/SR and/or the increase of resting $[Ca^{2+}]_c$ levels by Phe. Our data using native PAGE strongly support the idea that the MCU channel is a tetramer (see also (63)) and that the tetrameric assembly is augmented by Pyk2-mediated tyrosine phosphorylation (18) (Fig. 6), although Baughman *et al.* reported a larger complex (3). The difference between these two studies may be due to the distinct solubilization methods used, such that the larger complex may also include additional mtCU auxiliary proteins, such as MICU1(11). Further studies are needed to clarify whether tyrosine phosphorylation of MCU modulates the interaction of the channel pore with its regulatory proteins and changes its channel property such as Ca^{2+} sensitivity.

Role of MCU in ROS generation
and proapoptotic protein release

In this study, we found that α_1-AR-Pyk2-MCU signaling induced mROS generation (especially mSOF), proapoptotic protein release through mitochondrial Ca^{2+} overload, and

ultimately, initiating a classic apoptotic signaling cascade and cell death. In addition, α_1-AR-Pyk2-MCU-mediated mROS generation and mitochondrial release of proapoptotic proteins were prevented by either a potent FAK/Pyk2 inhibitor or expression of MCU-DN/MCUB. These findings raise the distinct possibility of targeting the Pyk2 activity as a novel therapeutic strategy to prevent mitochondrial Ca^{2+} overload, ROS generation, and cell injury (see also next section).

The alterations in mitochondrial Ca^{2+} homeostasis are frequently observed under cardiac pathological conditions (15, 16, 25), where AR signaling also exists (36). Recently, G$_q$PCR stimulation, including *via* α_1-AR, was shown to increase ROS in cardiomyocytes that activate ROS-sensitive downstream signaling processes (*e.g.*, Pyk2 and CaMKII) (21, 27). However, the detailed mechanism by which α_1-ARS induces oxidative stress is unclear. In this study, we confirmed that α_1-ARS increases ROS levels, as previously reported in native cardiomyocytes (70). Moreover, we showed that the main source of ROS generation during Phe stimulation is the mitochondria and Pyk2-MCU signaling is critical for mSO generation. We also demonstrated that mROS increases the Pyk2 activity and mitochondrial localization (Supplementary Fig. S9). These data also indicate that persistent α_1-ARS activates a vicious cycle of ROS-induced ROS generation (75) as a result of ROS-sensitive activation of Pyk2 (Fig. 10).

By being the primary source of cellular ROS production, mitochondria play a crucial role for ROS signaling both in physiological and pathophysiological conditions (51, 66, 71). With sustained elevations in [Ca^{2+}]$_{mt}$, mROS generation and $\Delta\Psi_{mt}$ depolarization trigger the mPTP opening that leads to apoptosis (7, 35). Thus, [Ca^{2+}]$_{mt}$ is commonly regarded as an important determinant in cell sensitivity to apoptotic stimuli in various cell types (64). Sites of intimate ER-mitochondria contact enable efficient local Ca^{2+} transmission between the two organelles, which serves as a potential regulatory site for apoptotic signaling (60), possibly *via* [Ca^{2+}]$_{mt}$-ROS-mPTP pathways (see Figs. 8–10). We reported that the mitochondrial voltage-dependent anion channel 1 (VDAC1) selectively interacts with the IP$_3$ receptor in the ER to direct the apoptotic Ca^{2+} release signals into mitochondria (13). Finally, we demonstrate here the direct involvement of Ca^{2+} influx through MCU in the regulation of mROS generation, apoptotic signaling, and cell death in native cardiomyocytes (Fig. 9).

In this study, a supraphysiological concentration of an α_1-AR agonist Phe (100 μM) was used for activating the cell death cascade to mimic the pathophysiological conditions (*e.g.*, chronic AR stimulation or a neurohumoral injury state). However, what is the physiological relevance of α_1-AR-Pyk2-MCU signaling? We also tested the concentration-dependent effect of Phe on [Ca^{2+}]$_{mt}$ elevation and found that Phe had a significant effect for activating mitochondrial Ca^{2+} uptake through MCU in the range of the subphysiological concentration (EC$_{50} \cong 2\,\mu M$) (Supplementary Fig. S5). We also showed that a significant reduction in the [Ca^{2+}]$_c$ transient was also observed, due to the increased Ca^{2+} clearance by mitochondria after α_1-ARS in H9C2 cells (Fig. 1E and Supplementary Fig. S5). These results are consistent with our previous observation that α_1-ARS decreases the Ca^{2+} transient by inhibiting (i) Ca^{2+} influx into the cell and (ii) by enhancing the Ca^{2+} clearance from the cytosol through PTK

activity (53). Recently, we proposed that MCU may serve as an important mechanism for cytosolic Ca^{2+} buffering when [Ca^{2+}]$_c$ increases at the ER/SR contact sites (17, 54). Therefore, physiological α_1-ARS may regulate/enhance the Ca^{2+} uptake by mitochondria, which may promote mitochondrial function and/or more efficient buffering of cytosolic Ca^{2+}. However, it is still controversial whether mitochondrial Ca^{2+} uptake contributes to the kinetics of beat-to-beat CaT formation in ACMs although mitochondria occupy 35% of cytosolic space and are well known to uptake Ca^{2+} (62). Shannon *et al.* estimated that the mitochondria contribute to only $\sim$1% of the total Ca^{2+} removal from the cytosol during CaT; SERCA and sarcolemmal Na^{2+}/Ca^{2+} exchanger (NCX) are responsible for almost all Ca^{2+} removal from the cytosol (69). Further studies are required for quantitatively evaluating the contribution of the α_1-AR-Pyk2-MCU signaling pathway for enhancing the mitochondrial Ca^{2+} buffering capacity during beat-to-beat CaT under AR stimulation.

α_1-AR-Pyk2 signaling as a novel therapeutic target for preventing mitochondrial Ca^{2+} overload, ROS generation, and cardiac injury

Pyk2 is abundantly found in various types of cancers and is well established as a key regulator of cancer proliferation, migration, and invasion (42, 42). Therefore, Pyk2 (or FAK) is a potent therapeutic target for cancer treatment, and currently, several FAK/Pyk2 inhibitors are already being evaluated in clinical trials (68). In cardiomyocytes, Pyk2 regulates the transcription factors that lead to cardiac remodeling, including hypertrophy (4, 29, 30). Therefore, Pyk2 is well studied as a component of nuclear signal transduction in cancer biology and cardiac remodeling. However, essentially, no information is available related to the effect of Pyk2 on mitochondrial functions. Interestingly, Pyk2 contains a predicted (using Mitoprot (10)) N-terminus mitochondria-targeting sequence (MSGVSEPLSRVKLGTLRRP), and a few reports have shown Pyk2 to be localized in mitochondria (1, 23). However, the functional role of mPyk2 has not been established. In this study, we confirmed that Pyk2 exists in the mitochondrial matrix in cardiac cells and found that α_1-ARS leads to activated Pyk2 translocation from the cytosol to mitochondrial matrix. Moreover, we showed that mPyk2 regulates MCU and initiates proapoptotic protein release from mitochondria. Although potent FAK/Pyk2 inhibitors (*e.g.*, PF-431396 and PF-562271) are widely used in the field of cancer research, there are no reports regarding the effects of these drugs in heart disease and mitochondrial injury. Our results suggest that the small-molecule Pyk2/FAK inhibitors or Pyk2 knockdown, may prevent mitochondrial Ca^{2+} overload, mROS generation, proapoptotic protein release, and cell death in the cardiomyocytes during sustained α_1-ARS or in the specific pathophysiological conditions where [Ca^{2+}]$_c$ overload and ROS overproduction coexist (*e.g.*, ischemic–reperfusion).

Recently, Pyk2 was shown to be activated in human no-ischemic heart failure (40). However, in heart failure, it has been well reported that there is a significant elevation of cytosolic Na^{2+} concentration ([Na^{2+}]$_c$), which enhanced cytosolic Ca^{2+} extrusion from the cell during diastole through NCX and reduced the [Ca^{2+}]$_c$ transient (52). In

addition, the $[Na^{2+}]_c$ elevation and mitochondrial NCX activity in heart failure dictate mROS generation through a decrease in the mitochondrial Ca^{2+} uptake (50). Indeed, several studies showed that mitochondrial Ca^{2+} uptake is reduced in failing cardiomyocytes (43, 47). These reports demonstrated that elevated $[Na^+]_c$ and mitochondrial NCX activity also critically contribute to decreased $[Ca^{2+}]_{mt}$, especially during heart failure. Since we did not observe the detailed relationship between the Pyk2-dependent MCU regulation and $[Na^{2+}]_c$ or resting $[Ca^{2+}]_c$ in this study, it is still not clear whether activated Pyk2 during heart failure has a significant impact on the MCU function.

Limitation of this study

In this study, most of the experiments were performed in cultured cell lines. While important experiments validate using native cardiomyocytes, we still need to take into account that our finding cannot be directly applicable to the *in vivo* situation. Animal models such as the neurohumoral injury model using the α_1-AR agonist will be indispensable for exploring the role of the cardiac α_1-AR-Pyk2-MCU signaling pathway in physiological and pathophysiological conditions *in vivo* as well as validating the Pyk2 inhibition as a possible novel therapeutic strategy for preventing mitochondrial injury and cell death.

Conclusion

This study is the first to investigate the regulation of MCU by cardiac adrenergic signaling. Elucidation of these regulatory mechanisms may lead to the design of novel targets for the pharmacological management of heart failure, where chronic adrenergic stimulation, mitochondrial injury, oxidative stress, and myocardial death are present.

Materials and Methods

An expanded fully described Materials and Methods section is available in Supplementary Data.

Cell cultures

H9c2 cells and HEK293T cells were maintained, transfected with plasmids, and used for experiments (37, 53, 54). HEK293T-MCU-Flag cells were generated by transecting with pcDNA3.1(+)-MCU-Flag and maintained in the presence of G-418 (53). NCMs and ACMs were isolated from Sprague-Dawley rats, plated, cultured, and used for experiments (37). NCMs were transfected with plasmids and ACMs were infected with adenovirus (17, 37). All animal experiments were performed in accordance with the Guideline on Animal Experimentation of Thomas Jefferson University (TJU). The study protocol was approved by the Animal Care Committee of TJU. The investigation conformed to the Guideline for the Care and Use of Laboratory Animals published by the US National Institutes of Health (NIH).

Mitochondrial protein isolation, Western immunoblot analysis, in vitro kinase, and binding assay

Whole cell lysates and mitochondria-enriched and cytosolic proteins were prepared (53). For electrophoresis under nondissociating conditions, mitochondrial proteins or whole cell lysates were separated by 10% polyacrylamide gel (Native-PAGE) (63). IP (37), *in vitro* binding (72), and kinase assays (37) were performed as described previously.

Live cell imaging in confocal microscopy and image analysis

The $[Ca^{2+}]_{mt}$ measurement using mitochondria-targeted Ca^{2+} biosensor Mitycam (39, 53), $[Ca^{2+}]_c$ measurement using Fura-Red (53), FRET measurement (63), mSO measurements by MitoSOX-Red (53), visualizing the release of mitochondrial intermembrane space proteins (49), measurement of mSOF by mT-cpYFP (73), detection of caspases 3/7 activity (48) were performed in live cells using the laser scanning confocal microscope (Olympus, Tokyo, Japan). There were no significant changes in the initial Mitycam fluorescence levels between the different experimental settings used in this study (see Supplementary Fig. S15). All images were analyzed with ImageJ software (NIH).

Data and statistical analysis

All results are shown as mean standard error. Unpaired Student's *t*-test was performed for two data sets. For multiple comparisons, one-way ANOVA followed by the *post hoc* Tukey test was performed. Statistical significance was set as a p value of <0.05.

Author Disclosure Statement

No competing financial interests exist.

References

1. Arcucci A, Montagnani S, and Gionti E. Expression and intracellular localization of Pyk2 in normal and v-src transformed chicken epiphyseal chondrocytes. *Biochimie* 88: 77–84, 2006.
2. Bagi CM, Christensen J, Cohen DP, Roberts WG, Wilkie D, Swanson T, Tuthill T, and Andresen CJ. Sunitinib and PF-562,271 (FAK/Pyk2 inhibitor) effectively block growth and recovery of human hepatocellular carcinoma in a rat xenograft model. *Cancer Biol Ther* 8: 856–865, 2009.
3. Baughman JM, Perocchi F, Girgis HS, Plovanich M, Belcher-Timme CA, Sancak Y, Bao XR, Strittmatter L, Goldberger O, Bogorad RL, Koteliansky V, and Mootha VK. Integrative genomics identifies MCU as an essential component of the mitochondrial calcium uniporter. *Nature* 476: 341–345, 2011.
4. Bayer AL, Heidkamp MC, Patel N, Porter MJ, Engman SJ, and Samarel AM. PYK2 expression and phosphorylation increases in pressure overload-induced left ventricular hypertrophy. *Am J Physiol Heart Circ Physiol* 283: H695–H706, 2002.
5. Blom N, Gammeltoft S, and Brunak S. Sequence and structure-based prediction of eukaryotic protein phosphorylation sites. *J Mol Biol* 294: 1351–1362, 1999.

6. Bonnette PC, Robinson BS, Silva JC, Stokes MP, Brosius AD, Baumann A, and Buckbinder L. Phosphoproteomic characterization of PYK2 signaling pathways involved in osteogenesis. *J Proteomics* 73: 1306–1320, 2010.

7. Brenner C and Moulin M. Physiological roles of the permeability transition pore. *Circ Res* 111: 1237–1247, 2012.

8. Carafoli E. Intracellular calcium homeostasis. *Annu Rev Biochem* 56: 395–433, 1987.

9. Chaudhuri D, Sancak Y, Mootha VK, and Clapham DE. MCU encodes the pore conducting mitochondrial calcium currents. *Elife* 2: e00704, 2013.

10. Claros MG and Vincens P. Computational method to predict mitochondrially imported proteins and their targeting sequences. *Eur J Biochem* 241: 779–786, 1996.

11. Csordas G, Golenar T, Seifert EL, Kamer KJ, Sancak Y, Perocchi F, Moffat C, Weaver D, de la Fuente Perez S, Bogorad R, Koteliansky V, Adijanto J, Mootha VK, and Hajnoczky G. MICU1 Controls Both the Threshold and Cooperative Activation of the Mitochondrial Ca(2+) Uniporter. *Cell Metab* 17: 976–987, 2013.

12. Dai S, Hall DD, and Hell JW. Supramolecular assemblies and localized regulation of voltage-gated ion channels. *Physiol Rev* 89: 411–452, 2009.

13. De Stefani D, Bononi A, Romagnoli A, Messina A, De Pinto V, Pinton P, and Rizzuto R. VDAC1 selectively transfers apoptotic Ca2+ signals to mitochondria. *Cell Death Differ* 19: 267–273, 2012.

14. De Stefani D, Raffaello A, Teardo E, Szabo I, and Rizzuto R. A forty-kilodalton protein of the inner membrane is the mitochondrial calcium uniporter. *Nature* 476: 336–340, 2011.

15. Dedkova EN and Blatter LA. Measuring mitochondrial function in intact cardiac myocytes. *J Mol Cell Cardiol* 52: 48–61, 2012.

16. Dedkova EN and Blatter LA. Mitochondrial Ca2+ and the heart. *Cell Calcium* 44: 77–91, 2008.

17. Drago I, De Stefani D, Rizzuto R, and Pozzan T. Mitochondrial Ca2+ uptake contributes to buffering cytoplasmic Ca2+ peaks in cardiomyocytes. *Proc Natl Acad Sci U S A* 109: 12986–12991, 2012.

18. Drago I, Pizzo P, and Pozzan T. After half a century mitochondrial calcium in- and efflux machineries reveal themselves. *EMBO J* 30: 4119–4125, 2011.

19. Duchen MR, Verkhratsky A, and Muallem S. Mitochondria and calcium in health and disease. *Cell Calcium* 44: 1–5, 2008.

20. Erickson JR, Joiner ML, Guan X, Kutschke W, Yang J, Oddis CV, Bartlett RK, Lowe JS, O'Donnell SE, Aykin-Burns N, Zimmerman MC, Zimmerman K, Ham AJ, Weiss RM, Spitz DR, Shea MA, Colbran RJ, Mohler PJ, and Anderson ME. A dynamic pathway for calcium-independent activation of CaMKII by methionine oxidation. *Cell* 133: 462–474, 2008.

21. Erickson JR, Patel R, Ferguson A, Bossuyt J, and Bers DM. Fluorescence resonance energy transfer-based sensor Camui provides new insight into mechanisms of calcium/calmodulin-dependent protein kinase II activation in intact cardiomyocytes. *Circ Res* 109: 729–738, 2011.

22. Frank GD, Mifune M, Inagami T, Ohba M, Sasaki T, Higashiyama S, Dempsey PJ, and Eguchi S. Distinct mechanisms of receptor and nonreceptor tyrosine kinase activation by reactive oxygen species in vascular smooth muscle cells: role of metalloprotease and protein kinase C-delta. *Mol Cell Biol* 23: 1581–1589, 2003.

23. Frazier DP, Wilson A, Dougherty CJ, Li H, Bishopric NH, and Webster KA. PKC-alpha and TAK-1 are intermediates in the activation of c-Jun NH2-terminal kinase by hypoxia-reoxygenation. *Am J Physiol Heart Circ Physiol* 292: H1675–H1684, 2007.

24. Giacomello M, Drago I, Pizzo P, and Pozzan T. Mitochondrial Ca2+ as a key regulator of cell life and death. *Cell Death Differ* 14: 1267–1274, 2007.

25. Griffiths EJ. Mitochondria and heart disease. *Adv Exp Med Biol* 942: 249–267, 2012.

26. Gunter TE and Pfeiffer DR. Mechanisms by which mitochondria transport calcium. *Am J Physiol* 258: C755–C786, 1990.

27. Guo J, Sabri A, Elouardighi H, Rybin V, and Steinberg SF. Alpha1-adrenergic receptors activate AKT via a Pyk2/PDK-1 pathway that is tonically inhibited by novel protein kinase C isoforms in cardiomyocytes. *Circ Res* 99: 1367–1375, 2006.

28. Hebert-Chatelain E. Src kinases are important regulators of mitochondrial functions. *Int J Biochem Cell Biol* 45: 90–98, 2013.

29. Heidkamp MC, Scully BT, Vijayan K, Engman SJ, Szotek EL, and Samarel AM. PYK2 regulates SERCA2 gene expression in neonatal rat ventricular myocytes. *Am J Physiol Cell Physiol* 289: C471–C482, 2005.

30. Hirotani S, Higuchi Y, Nishida K, Nakayama H, Yamaguchi O, Hikoso S, Takeda T, Kashiwase K, Watanabe T, Asahi M, Taniike M, Tsujimoto I, Matsumura Y, Sasaki T, Hori M, and Otsu K. Ca(2+)-sensitive tyrosine kinase Pyk2/CAK beta-dependent signaling is essential for G-protein-coupled receptor agonist-induced hypertrophy. *J Mol Cell Cardiol* 36: 799–807, 2004.

31. Hom J, Yu T, Yoon Y, Porter G, and Sheu SS. Regulation of mitochondrial fission by intracellular Ca2+ in rat ventricular myocytes. *Biochim Biophys Acta* 1797: 913–921, 2010.

32. Hornbeck PV, Chabra I, Kornhauser JM, Skrzypek E, and Zhang B. PhosphoSite: a bioinformatics resource dedicated to physiological protein phosphorylation. *Proteomics* 4: 1551–1561, 2004.

33. Hornbeck PV, Kornhauser JM, Tkachev S, Zhang B, Skrzypek E, Murray B, Latham V, and Sullivan M. PhosphoSitePlus: a comprehensive resource for investigating the structure and function of experimentally determined post-translational modifications in man and mouse. *Nucleic Acids Res* 40: D261–D270, 2012.

34. Jahnel U, Nawrath H, Shieh RC, Sharma VK, Williford DJ, and Sheu SS. Modulation of cytosolic free calcium concentration by alpha 1-adrenoceptors in rat atrial cells. *Naunyn Schmiedebergs Arch Pharmacol* 346: 88–93, 1992.

35. Javadov S, Karmazyn M, and Escobales N. Mitochondrial permeability transition pore opening as a promising therapeutic target in cardiac diseases. *J Pharmacol Exp Ther* 330: 670–678, 2009.

36. Jensen BC, O'Connell TD, and Simpson PC. Alpha-1-adrenergic receptors: targets for agonist drugs to treat heart failure. *J Mol Cell Cardiol* 51: 518–528, 2011.

37. Jhun BS, O-Uchi J, Wang W, Ha CH, Zhao J, Kim JY, Wong C, Dirksen RT, Lopes CM, and Jin ZG. Adrenergic signaling controls RGK-dependent trafficking of cardiac voltage-gated L-type Ca2+ channels through PKD1. *Circ Res* 110: 59–70, 2012.

38. Joiner ML, Koval OM, Li J, He BJ, Allamargot C, Gao Z, Luczak ED, Hall DD, Fink BD, Chen B, Yang J, Moore

SA, Scholz TD, Strack S, Mohler PJ, Sivitz WI, Song LS, and Anderson ME. CaMKII determines mitochondrial stress responses in heart. *Nature* 491: 269–273, 2012.

39. Kettlewell S, Cabrero P, Nicklin SA, Dow JA, Davies S, and Smith GL. Changes of intra-mitochondrial Ca2+ in adult ventricular cardiomyocytes examined using a novel fluorescent Ca2+ indicator targeted to mitochondria. *J Mol Cell Cardiol* 46: 891–901, 2009.

40. Lang D, Glukhov AV, Efimova T, and Efimov IR. Role of Pyk2 in cardiac arrhythmogenesis. *Am J Physiol Heart Circ Physiol* 301: H975–H983, 2011.

41. Lax A, Soler F, and Fernandez-Belda F. Intracellular ca(2+) pools and fluxes in cardiac muscle-derived h9c2 cells. *J Bioenerg Biomembr* 37: 249–259, 2005.

42. Lipinski CA and Loftus JC. Targeting Pyk2 for therapeutic intervention. *Expert Opin Ther Targets* 14: 95–108, 2010.

43. Liu T and O'Rourke B. Enhancing mitochondrial Ca2+ uptake in myocytes from failing hearts restores energy supply and demand matching. *Circ Res* 103: 279–288, 2008.

44. Lopez JR, Espinosa R, Landazuru P, Linares N, Allen P, and Mijares A. Dysfunction of diastolic [Ca(2)(+)] in cardiomyocytes isolated from chagasic patients. *Rev Esp Cardiol* 64: 456–462, 2011.

45. Luo DL, Gao J, Fan LL, Tang Y, Zhang YY, and Han QD. Receptor subtype involved in alpha 1-adrenergic receptor-mediated Ca2+ signaling in cardiomyocytes. *Acta Pharmacol Sin* 28: 968–974, 2007.

46. Martell JD, Deerinck TJ, Sancak Y, Poulos TL, Mootha VK, Sosinsky GE, Ellisman MH, and Ting AY. Engineered ascorbate peroxidase as a genetically encoded reporter for electron microscopy. *Nat Biotechnol* 30: 1143–1148, 2012.

47. Michels G, Khan IF, Endres-Becker J, Rottlaender D, Herzig S, Ruhparwar A, Wahlers T, and Hoppe UC. Regulation of the human cardiac mitochondrial Ca2+ uptake by 2 different voltage-gated Ca2+ channels. *Circulation* 119: 2435–2443, 2009.

48. Miyata M, Kambe M, Tajima O, Moriya S, Sawaki H, Hotta H, Kondo Y, Narimatsu H, Miyagi T, Furukawa K, and Furukawa K. Membrane sialidase NEU3 is highly expressed in human melanoma cells promoting cell growth with minimal changes in the composition of gangliosides. *Cancer Sci* 102: 2139–2149, 2011.

49. Munoz-Pinedo C, Guio-Carrion A, Goldstein JC, Fitzgerald P, Newmeyer DD, and Green DR. Different mitochondrial intermembrane space proteins are released during apoptosis in a manner that is coordinately initiated but can vary in duration. *Proc Natl Acad Sci U S A* 103: 11573–11578, 2006.

50. Nickel A, Loffler J, and Maack C. Myocardial energetics in heart failure. *Basic Res Cardiol* 108: 358, 2013.

51. O'Rourke B, Cortassa S, and Aon MA. Mitochondrial ion channels: gatekeepers of life and death. *Physiology (Bethesda)* 20: 303–315, 2005.

52. O'Rourke B and Maack C. The role of Na dysregulation in cardiac disease and how it impacts electrophysiology. *Drug Discov Today Dis Models* 4: 207–217, 2007.

53. O-Uchi J, Jhun BS, Hurst S, Bisetto S, Gross P, Chen M, Kettlewell S, Park J, Oyamada H, Smith GL, Murayama T, and Sheu SS. Overexpression of ryanodine receptor type 1 enhances mitochondrial fragmentation and Ca2+ -induced ATP production in cardiac H9c2 myoblasts. *Am J Physiol Heart Circ Physiol* 305: H1736–H1751, 2013.

54. O-Uchi J, Komukai K, Kusakari Y, Morimoto S, Kawai M, Jhun BS, Hurst S, Hongo K, Sheu SS, and Kurihara S. Alpha-adrenenoceptor stimulation inhibits cardiac excitation-contraction coupling through tyrosine phosphorylation of beta-adrenoceptor. *Biochem Biophys Res Commun* 433: 188–193, 2013.

55. O-Uchi J and Lopes CM. Combined blockade of beta- and alpha(1)-adrenoceptors in left ventricular remodeling induced by hypertension: beneficial or not? *Hypertens Res* 33: 984–985, 2010.

56. O-Uchi J, Pan S, and Sheu SS. Perspectives on: SGP Symposium on Mitochondrial Physiology and Medicine: Molecular identities of mitochondrial Ca2+ influx mechanism: Updated passwords for accessing mitochondrial Ca2+ -linked health and disease. *J Gen Physiol* 139: 435–443, 2012.

57. O-Uchi J, Ryu S-Y, Jhun BS, Hurst S, and Sheu S-S. Mitochondrial ion channels/transporters as sensors and regulators of cellular redox signaling. *Antioxid Redox Signal* 21: 987–1006, 2014.

58. O-Uchi J, Sasaki H, Morimoto S, Kusakari Y, Shinji H, Obata T, Hongo K, Komukai K, and Kurihara S. Interaction of alpha1-adrenoceptor subtypes with different G proteins induces opposite effects on cardiac L-type Ca2+ channel. *Circ Res* 102: 1378–1388, 2008.

59. Paillard M, Tubbs E, Thiebaut PA, Gomez L, Fauconnier J, Da Silva CC, Teixeira G, Mewton N, Belaidi E, Durand A, Abrial M, Lacampagne A, Rieusset J, and Ovize M. Depressing mitochondria-reticulum interactions protects cardiomyocytes from lethal hypoxia-reoxygenation injury. *Circulation* 128: 1555–1565, 2013.

60. Pinton P, Ferrari D, Rapizzi E, Di Virgilio F, Pozzan T, and Rizzuto R. The Ca2+ concentration of the endoplasmic reticulum is a key determinant of ceramide-induced apoptosis: significance for the molecular mechanism of Bcl-2 action. *EMBO J* 20: 2690–2701, 2001.

61. Prasad AM and Inesi G. Effects of thapsigargin and phenylephrine on calcineurin and protein kinase C signaling functions in cardiac myocytes. *Am J Physiol Cell Physiol* 296: C992–C1002, 2009.

62. Prosser BL, Ward CW, and Lederer WJ. Subcellular Ca2+ signaling in the heart: the role of ryanodine receptor sensitivity. *J Gen Physiol* 136: 135–142, 2010.

63. Raffaello A, De Stefani D, Sabbadin D, Teardo E, Merli G, Picard A, Checchetto V, Moro S, Szabo I, and Rizzuto R. The mitochondrial calcium uniporter is a multimer that can include a dominant-negative pore-forming subunit. *EMBO J* 32: 2362–2376, 2013.

64. Rizzuto R, Marchi S, Bonora M, Aguiari P, Bononi A, De Stefani D, Giorgi C, Leo S, Rimessi A, Siviero R, Zecchini E, and Pinton P. Ca(2+) transfer from the ER to mitochondria: when, how and why. *Biochim Biophys Acta* 1787: 1342–1351, 2009.

65. Roberts WG, Ung E, Whalen P, Cooper B, Hulford C, Autry C, Richter D, Emerson E, Lin J, Kath J, Coleman K, Yao L, Martinez-Alsina L, Lorenzen M, Berliner M, Luzzio M, Patel N, Schmitt E, LaGreca S, Jani J, Wessel M, Marr E, Griffor M, and Vajdos F. Antitumor activity and pharmacology of a selective focal adhesion kinase inhibitor, PF-562,271. *Cancer Res* 68: 1935–1944, 2008.

66. Santos CX, Anilkumar N, Zhang M, Brewer AC, and Shah AM. Redox signaling in cardiac myocytes. *Free Radic Biol Med* 50: 777–793, 2011.

67. Sayas CL, Ariaens A, Ponsioen B, and Moolenaar WH. GSK-3 is activated by the tyrosine kinase Pyk2 during LPA1-mediated neurite retraction. *Mol Biol Cell* 17: 1834–1844, 2006.

68. Schultze A and Fiedler W. Clinical importance and potential use of small molecule inhibitors of focal adhesion kinase. *Anticancer Agents Med Chem* 11: 593–599, 2011.

69. Shannon TR, Wang F, Puglisi J, Weber C, and Bers DM. A mathematical treatment of integrated Ca dynamics within the ventricular myocyte. *Biophys J* 87: 3351–3371, 2004.

70. Tanaka K, Honda M, and Takabatake T. Redox regulation of MAPK pathways and cardiac hypertrophy in adult rat cardiac myocyte. *J Am Coll Cardiol* 37: 676–685, 2001.

71. Tsutsui H, Kinugawa S, and Matsushima S. Oxidative stress and heart failure. *Am J Physiol Heart Circ Physiol* 301: H2181–H2190, 2011.

72. Ueki S, Lacroix B, and Citovsky V. Protein membrane overlay assay: a protocol to test interaction between soluble and insoluble proteins *in vitro*. *J Vis Exp* 54: pii: 2961, 2011.

73. Wang W, Fang H, Groom L, Cheng A, Zhang W, Liu J, Wang X, Li K, Han P, Zheng M, Yin J, Wang W, Mattson MP, Kao JP, Lakatta EG, Sheu SS, Ouyang K, Chen J, Dirksen RT, and Cheng H. Superoxide flashes in single mitochondria. *Cell* 134: 279–290, 2008.

74. Xue Y, Ren J, Gao X, Jin C, Wen L, and Yao X. GPS 2.0, a tool to predict kinase-specific phosphorylation sites in hierarchy. *Mol Cell Proteomics* 7: 1598–1608, 2008.

75. Zorov DB, Juhaszova M, and Sollott SJ. Mitochondrial ROS-induced ROS release: an update and review. *Biochim Biophys Acta* 1757: 509–517, 2006.

Address correspondence to:
Dr. Jin O-Uchi
Department of Medicine
Center for Translational Medicine
Jefferson Medical College
Thomas Jefferson University
1020 Locust Street, Suite 543G
Philadelphia, PA 19107

E-mail: jin.ouchi@jefferson.edu

Dr. Shey-Shing Sheu
Department of Medicine
Center for Translational Medicine
Jefferson Medical College
Thomas Jefferson University
1025 Locust Street, Suite 543D
Philadelphia, PA 19107

E-mail: shey-shing.sheu@jefferson.edu

Abbreviations Used

α_1-AR = α_1-adrenoceptor
α_1-ARS = α_1-adrenoceptor stimulation
$\Delta\Psi_m$ = mitochondrial membrane potential
ACM = isolated adult cardiomyocytes
$[Ca^{2+}]_c$ = cytosolic Ca^{2+} concentration
$[Ca^{2+}]_{mt}$ = mitochondrial matrix Ca^{2+} concentration
CaMKII = Ca^{2+}/calmodulin-dependent protein kinase II
CCDC109A = coiled-coil domain-containing protein 109A
Cyp-D = cyclophilin D
DN = dominant negative
ER = endoplasmic reticulum
FAK = focal adhesion kinase
FCCP = carbonyl cyanide 4-(trifluoromethoxy) phenylhydrazone
FRET = Förster resonance energy transfer
G_qPCR = G_q-protein coupling receptor
HEK293T-MCU-Flag cells = HEK293T cells stably overexpressing MCU-Flag
IMM = inner mitochondrial membranes
IP = immunoprecipitation
KD = kinase dead
MCU = mitochondrial Ca^{2+} uniporter pore
mPTP = mitochondrial permeability transition pore
mPyk2 = mitochondrial Pyk2
mROS = ROS production in mitochondria
mSO = mitochondrial superoxide
mSOF = mitochondrial superoxide flashes
mtCU = mitochondrial Ca^{2+} uniporter
mt-RFP = mitochondria-targeted RFP
NCM = neonatal cardiomyocyte
OMM = outer mitochondrial membranes
Phe = phenylephrine
PK = Proteinase K
P-Tyr = phosphotyrosine
Pyk2 = proline-rich tyrosine kinase 2
ROS = reactive oxygen species
SERCA = sarcoendoplasmic reticulum/ endoplasmic reticulum Ca^{2+}-ATPase
Smac = second mitochondrial-derived activator of caspases
SR = sarcoplasmic reticulum
TG = thapsigargin
VDAC = voltage-dependent anion channel
WCL = whole cell lysates